A LOCALIZATION STRATEGY FOR DATA ASSIMILATION; APPLICATION TO STATE ESTIMATION AND PARAMETER ESTIMATION*

TOMMASO TADDEI† AND ANTHONY T. PATERA‡

Abstract. We present a localization procedure for addressing data assimilation tasks — state estimation and parameter estimation — in which the quantity of interest pertains to a subregion of the domain over which the mathematical model is properly defined. Given the domain Ω^{pb} associated with the full system, and the domain of interest $\Omega \subset \Omega^{\text{pb}}$, our localization procedure relies on the definition of an intermediate domain Ω^{bk} such that $\bar{\Omega} \subset \bar{\Omega}^{\text{bk}} \subset \bar{\Omega}^{\text{pb}}$. The domain Ω^{bk} is chosen to exclude many parameters associated with the parametrization of the mathematical model in $\Omega^{\text{pb}} \setminus \Omega$ and to thereby reduce the difficulty of the estimation problem. Our approach exploits a Model-Order-Reduction (MOR) procedure to properly address (i) uncertainty in the value of the parameters in Ω, and (ii) uncertainty in the boundary conditions at the interface between Ω^{bk} and $\Omega^{\text{pb}} \setminus \Omega^{\text{bk}}$. We present theoretical results to demonstrate the optimality of our construction. We further present two numerical synthetic examples in acoustics to demonstrate the effectiveness of our localization procedure in reducing uncertainty dimensionality, and thus in simplifying the data assimilation task.

Key words. data assimilation, inverse problems, model order reduction

AMS subject classifications. 6207, 65M32, 93E24

1. Introduction.

In practical applications, best-knowledge (bk) mathematical models might be characterized by extremely high-dimensional parametric uncertainty. In the process of defining the model, we must indeed specify potential variations in the topology of the structure, material properties, and initial and boundary conditions, just to mention a few; since all these quantities are typically subject to uncertainty, the effective number of parameters associated with the mathematical model of a full engineering system might number in the hundreds.

In many cases, we are interested in the solution to the mathematical model — which in this paper corresponds to a Partial Differential Equation (PDE) — in a subregion of the whole system: for acoustic applications, active systems for noise cancellation rely on the estimation of the sound pressure level in a particular region of interest; in damage identification, engineers are often able to anticipate the region of the structure of interest that is more likely prone to failure, and consequently monitor only these parts of the structure. Once we restrict the model to the subregion of interest, we must face two different sources of uncertainty in the model: (i) uncertainty in the physical parameters within the subregion, and (ii) uncertainty in the boundary conditions at the (artificial) interface — following [21], we here refer to model uncertainty as to the uncertainty in the value of the parameters (parametric uncertainty) and/or in source term and boundary conditions (non-parametric uncertainty). While we might reasonably assume that the former source of uncertainty leads to a low-dimensional parametrization, the latter clearly leads to a high-dimensional and possibly infinite-dimensional parameter space.

To address the uncertainty related to boundary conditions, we propose a two-stage localization procedure. If we denote by Ω^{pb} the domain associated with the full

*Submitted to the editors September 23, 2019.

Funding: This work was funded by ONR Grant N00014-11-1-0713.

†Laboratoire Jacques-Louis Lions, Université Pierre et Marie Curie, Paris, France (taddei@ljll.math.upmc.fr).

‡Department of Mechanical Engineering, MIT, Cambridge, MA, USA (patera@mit.edu).

system, and by $\Omega \subset \Omega^{\rm pb}$ the domain of interest, we introduce the bk domain $\Omega^{\rm bk}$ such that $\bar{\Omega} \subset \bar{\Omega}^{\rm bk} \subset \bar{\Omega}^{\rm pb}$, where $\bar{S}$ denotes the closure of the set S, $S = \Omega, \Omega^{\rm bk}, \Omega^{\rm pb}$. We denote by $\Gamma^{\rm in} \subset \partial\Omega^{\rm bk}$ the interface between the domain $\Omega^{\rm pb} \setminus \Omega^{\rm bk}$ and the domain $\Omega^{\rm bk}$ in which boundary conditions are uncertain. The domain $\Omega^{\rm bk}$ is chosen to exclude many parameters associated with $\Omega^{\rm pb} \setminus \Omega$; however, we must also ensure that $\Gamma^{\rm in}$ is separated from Ω, that is $\text{dist}(\Omega, \Gamma^{\rm in}) > 0$. We further denote by $\mu \in \mathcal{P}$ the parameters active in $\Omega^{\rm bk}$, and by $g \in \mathcal{T}$ the unknown restriction of the true state to the interface $\Gamma^{\rm in}$: here, the parameter space $\mathcal{P} \subset \mathbb{R}^P$ represents a "confidence region" for the true value of μ, while $\mathcal{T}$ is a suitable functional space defined over $\Gamma^{\rm in}$. Exploiting the previous definitions, we finally introduce the bk solution map $(g, \mu) \in \mathcal{T} \times \mathcal{P} \mapsto u_g(\mu) \in \mathcal{V}$, where $\mathcal{V}$ is a suitable Hilbert space over $\Omega^{\rm bk}$: $u_g(\mu)$ is the solution to the μ-parametrized bk differential equation in $\Omega^{\rm bk}$ with Dirichlet boundary condition g on $\Gamma^{\rm in}$. Figure 1 shows two possible instances of the localization strategy proposed in this paper.

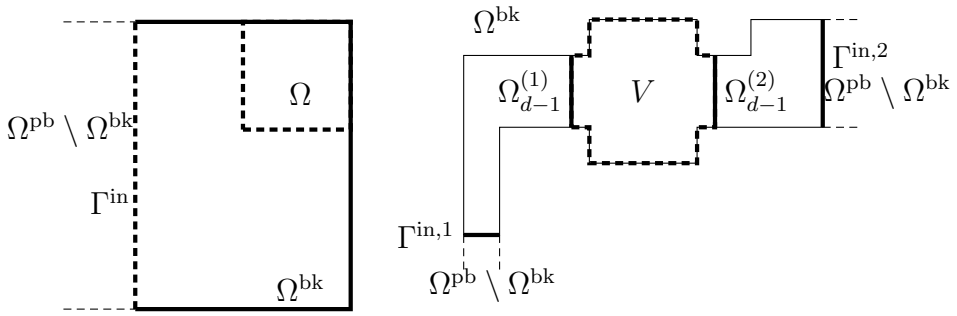

(a) state estimation (b) parameter estimation

Fig. 1: Localization strategy. Figure (a): state estimation in Ω. Figure (b): parameter estimation in V.

In this work, we propose and analyse a Model-Order-Reduction (MOR) procedure for the construction of hierarchical local approximation spaces $\mathcal{Z}_1 \subset \ldots \subset \mathcal{Z}_{N_{\max}} \subset \mathcal{Y}$ for the restriction of the solution manifold to the domain of interest, $\{u_g(\mu)|_\Omega : g \in \mathcal{T},\ \mu \in \mathcal{P}\} \subset \mathcal{Y}$, where $\mathcal{Y}$ is a suitable Hilbert space on Ω. For $\mathcal{P} = \{\bar{\mu}\}$ (a parameter singleton), we define the space $\mathcal{Z}_N$ as the span of the first N eigenmodes of a transfer eigenproblem ([27]). For $\mathcal{P} \neq \{\bar{\mu}\}$, we first build separately $n_{\rm train}$ approximation spaces $\mathcal{Z}_N^{(1)}, \ldots, \mathcal{Z}_N^{(n_{\rm train})}$ associated with $n_{\rm train}$ different values of the parameter μ, $\{\mu^i\}_{i=1}^{n_{\rm train}}$, and then we condense these spaces into a single approximation space by applying a Proper Orthogonal Decomposition based on the method of snapshots (POD, [3, 20, 33]). Our approach is applicable to a large class of elliptic linear PDEs for both two-dimensional and three-dimensional domains. We can also consider the case in which the global domain $\Omega^{\rm bk}$ is of dimension d and the local domain Ω is of dimension $d-1$; if the domain of interest is $(d-1)$-dimensional, we use the notation Ω_{d-1}. For $\mathcal{P} = \{\bar{\mu}\}$, and second-order PDEs, we prove that our approach is optimal in a suitable Sobolev norm — $H^1(\Omega)$ if $\Omega \subset \mathbb{R}^d$, $H^{1/2}(\Omega_{d-1})$ if $\Omega_{d-1} \subset \mathbb{R}^{d-1}$ — in the sense of Kolmogorov.

Our localization strategy relies on the filtering properties of the differential operator associated with the mathematical model. From a physical standpoint, this is

closely connected to the concept of evanescence ([5]). For elliptic problems, if Γ^{in} is sufficiently far from the domain of interest Ω, we anticipate an exponential decay of the high-order modes of the Dirichlet boundary conditions at Γ^{in}. This effectively reduces the dimensionality of the solution manifold and permits its approximation through a low-dimensional linear space. We emphasize that the *reducibility* of the solution manifold is an intrinsic feature of the particular differential problem and system configuration at hand: in [36, Chapter 5.1.2] an example of a semi-infinite waveguide ([13]) is presented to show that the localization strategy relies on the assumption that the Kolmogorov N-width associated with the localized solution manifold decays sufficiently fast. *A priori* estimates for the decay of the Kolmogorov N-width of local solution manifolds are limited to the diffusion equation ([2, Theorem 3.3]): therefore, the reducibility of the manifold should be assessed on a case-by-case basis.

We apply our localization strategy to state estimation within the framework of the Parametrized-Background Data-Weak approach (PBDW, [21, 22]). Given M measurements $\ell_1^{\text{obs}}, \dots, \ell_M^{\text{obs}} \in \mathbb{C}$ in the domain Ω, we aim to estimate the state u^{true} over Ω. PBDW formulation seeks an approximation $u^\star = z^\star + \eta^\star$ to the true field u^{true} over Ω employing projection-by-data based on M measurements $\{\ell_m^{\text{obs}}\}_{m=1}^M$ of the form $\ell_m^{\text{obs}} = \ell_m^o(u^{\text{true}})$, where $\ell_1^o, \dots, \ell_M^o \in \mathcal{Y}'$ are suitably-chosen linear functionals associated with the physical transducers. The first contribution to $u^\star$, $z^\star \in \mathcal{Z}_N$, is the "deduced background estimate": since $\mathcal{Z}_N \subset \mathcal{Y}$ is informed by the bk solution manifold $\mathcal{M}$, $z^\star$ incorporates our prior knowledge of the state. The second contribution to $u^\star$, $\eta^\star \in \mathcal{Z}_N^\perp$, is the "update estimate": $\eta^\star$ is a linear combination of the Riesz representations of the M observation functionals $\{\ell_m^o\}_{m=1}^M$, and is designed to address the deficiencies of the bk model. The approach has been extended to pointwise noisy measurements in [35]. As discussed in the above-mentioned papers, the PBDW formulation is well-posed only if $N \le M$: for this reason, it is key to construct spaces $\{\mathcal{Z}_N\}_N$ that accurately approximate the solution manifold in Ω for moderate values of N. This motivates the use of our localization strategy for the determination of the background space $\mathcal{Z}_N$.

We also apply our localization strategy to parameter estimation. Given M direct and indirect measurements $\{\ell_m^{\text{obs}}\}_{m=1}^M$ of the state u^{true} in the domain $V \subset \Omega^{\text{pb}}$, parameter estimation techniques aim to approximate the parameter $\mu^\star \in \mathcal{P}$ associated with the current system. The state — and thus the observations — typically is not uniquely determined by the local parameters μ, but might also depend on other parameters associated with the domain $\Omega^{\text{pb}} \setminus V$, which might be difficult to characterize or might lead to an extremely high-dimensional parametrization. For this reason, the resulting inverse problem will be extremely difficult to solve, typically always ill-posed. This motivates the use of our localization procedure: first, we define (i) Ω^{bk} such that $V \subset \Omega^{\text{bk}} \subset \Omega^{\text{pb}}$, (ii) Ω_{d-1} as the intersection between ∂V and $\Omega^{\text{pb}} \setminus V$, and (iii) the possibly high-dimensional uncertainty set $\mathcal{T}$ on Γ^{in}; then, we employ our MOR technique to define an N-dimensional expansion for the restriction $\bar{g}$ of the state u to Ω_{d-1}. We can then consider the restriction of the state to V as a function of $\bar{g}$ and of the parameter μ. We refer to Figure 1(b) for a graphical explanation of the localization procedure. If N is modest compared to the global parametrization of the differential model, this approach dramatically reduces the dimensionality of the inverse problem.

The idea of employing a two-stage localization procedure based on the definition of an *intermediate* domain Ω^{bk}, $\Omega \subset \Omega^{\text{bk}} \subset \Omega^{\text{pb}}$, is new in the field of Data Assimilation. We remark that in Acoustics several authors have studied the problem of estimating the acoustic pressure in a domain Ω based on local measurements, under

the assumption that the pressure field satisfies the Helmholtz equation in a domain $\Omega^{\rm pb}$ containing Ω ([28, 39]). Chardon et al. ([8]) and Moiola et al. ([25]) apply Fourier-Bessel and plane-wave expansions to estimate the pressure field, and exploit the fact that the pressure satisfies the Helmholtz equation for a specific value of the wave number to derive *a priori* error estimates for the best-fit error in Sobolev norms. While these approaches rely on explicit expansions, we employ here an empirical basis which relies on the definition of the intermediate domain $\Omega^{\rm bk}$. Approaches based on explicit expansions are specialized to a specific parameter-independent equation, and to specific choices of the domain Ω; on the other hand, our approach is applicable to a wide class of equations and domains of interest, is guaranteed to be optimal in the sense of Kolmogorov, and can also address the case in which the PDE model contains uncertain parameters.

Our localization strategy is similar to the concept of oversampling in numerical multiscale methods ([18, 11, 15]). If we denote by $\mathcal{T}_H = \{T_i\}_{i=1}^{n_{\rm elem}}$ the *coarse mesh* of $\Omega^{\rm pb}$, oversampling methods consist (i) in defining and solving a suitable local problem for the coarse element T_i in the *patch* $U(T_i)$, $T_i \subset U(T_i) \subset \Omega^{\rm pb}$, and (ii) in restricting the solution to the local problem to the element T_i: the element T_i plays the role of Ω, and the patch $U(T_i)$ plays the role of $\Omega^{\rm bk}$. We remark that while our localization approach aims at reducing model uncertainty for data assimilation applications, oversampling aims at reducing the effect of resonance errors associated with the multiscale formulation.

Computational procedures for the construction of local approximation spaces based on the eigenmodes of a transfer eigenproblem are new in the context of data assimilation, but have already been exploited in several other applications. The transfer eigenproblem was first introduced and studied in the approximation theory literature (see, e.g., [27]). More recently, Babuška and Lipton in [2] employed the transfer eigenmodes to define local approximation spaces in the framework of the Generalized Finite Element method ([24, 1]). Smetana and Patera in [34] exploited the eigenmodes associated with the transfer eigenproblem in the context of Port-Reduced Static Condensation Reduced Basis Element (PR-scRBE, [19, 12]) Method for linear elasticity; furthermore, they proposed a Greedy technique to address the parametric dependence. More recently, Buhr and Smetana in [7] proposed to estimate the transfer eigenmodes based on random sampling of the boundary conditions.

In this work, we extend the analysis presented in [2] and [34] to a wide class of linear elliptic PDEs, and we also study the stability of the approach with respect to the choice of the finite-dimensional discretization $\mathcal{T}_{\mathcal{N}_{\rm in}}$ of $\mathcal{T}$ (cf. Proposition 3.5). Furthermore, we rigorously show that for $\mathcal{P} = \{\bar{\mu}\}$ the eigenmodes of the transfer eigenproblem correspond to the POD eigenmodes for a proper choice of the snapshots. The connection with POD allows us to interpret the combination of the transfer eigenproblem for fixed parameter with POD for parameter variation as a Hierarchical Approximate Proper Orthogonal Decomposition (HAPOD, [17, 26]). Using terminology introduced in [17], our approach corresponds to a *distributed approximated POD*. We exploit this connection in the analysis.

The paper is organized as follows. In section 2, we introduce our model reduction (data compression) strategy. In section 3, we present a number of theoretical results concerning the optimality of our construction. Then, we illustrate our localization strategy for state estimation (section 4), and for parameter estimation (section 5), through the vehicle of two acoustics examples. Finally, in section 6, we draw some conclusions.

2. Methodology.

2.1. Preliminaries. Let $\Omega^{\rm bk} \subset \mathbb{R}^d$ be a Lipschitz domain, and let $\Gamma^{\rm in} \subset \partial\Omega^{\rm bk}$ be an open set. Let Ω be either a d-dimensional open subset of $\Omega^{\rm bk}$, or a $d-1$-dimensional open subset of $\bar{\Omega}^{\rm bk}$; let us assume that $\mathrm{dist}(\Omega, \Gamma^{\rm in}) > 0$. We define the Hilbert spaces $\mathcal{V} = \mathcal{V}(\Omega^{\rm bk})$, $\mathcal{T} = \mathcal{T}(\Gamma^{\rm in})$, and $\mathcal{Y} = \mathcal{Y}(\Omega)$ endowed with the inner products $(\cdot,\cdot)_{\mathcal{V}}$, $(\cdot,\cdot)_{\mathcal{T}}$ and $(\cdot,\cdot)_{\mathcal{Y}}$, and the induced norms $\|\cdot\|_{\mathcal{V}}$, $\|\cdot\|_{\mathcal{T}}$, and $\|\cdot\|_{\mathcal{Y}}$, respectively. We also denote by $\Pi^{\mathcal{Y}}_{\mathcal{Q}}(\cdot)$ the projection operator onto $\mathcal{Q} \subset \mathcal{Y}$ in $\mathcal{Y}$, and by $\Pi^{\mathcal{T}}_{\mathcal{Q}'}(\cdot)$ the projection operator onto $\mathcal{Q}' \subset \mathcal{T}$ in $\mathcal{T}$. Finally, we introduce the parameter space $\mathcal{P}$, which is assumed to be compact in $\mathbb{R}^P$. We remark that, in the data assimilation context, $\mathcal{P}$ represents a confidence region for the true value of μ associated with the state.

Given $g \in \mathcal{T}$ and $\mu \in \mathcal{P}$, we denote by $u_g(\mu) \in \mathcal{V}$ the unique solution to the variational problem

$$\mathcal{G}^\mu(u_g(\mu), v) = f(v), \quad \forall\, v \in \mathcal{V}_0, \quad u_g|_{\Gamma^{\rm in}} = g, \qquad \mu \in \mathcal{P}, \quad g \in \mathcal{T}, \tag{1}$$

where $\mathcal{V}_0 := \{v \in \mathcal{V} : v|_{\Gamma^{\rm in}} \equiv 0\}$, and $\mathcal{G}^\mu$ is an inf-sup stable bilinear form on $\mathcal{V}_0 \times \mathcal{V}_0$. In the remainder of this paper, we assume that for any value of $\mu \in \mathcal{P}$ and for any $g \in \mathcal{T}$ problem (1) is well-posed in $\mathcal{V}$, and $u_g(\mu)|_\Omega$ belongs to $\mathcal{Y}$. For simplicity, with no loss of generality, we assume that $f \equiv 0$. We further introduce the solution maps $\widehat{A} : \mathcal{T} \times \mathcal{P} \to \mathcal{V}$ and $A : \mathcal{T} \times \mathcal{P} \to \mathcal{Y}$ such that

$$\widehat{A}(g;\mu) = u_g(\mu), \quad A(g;\mu) = u_g(\mu)|_\Omega, \qquad \forall\, g \in \mathcal{T}, \quad \mu \in \mathcal{P}. \tag{2}$$

Due to the assumptions on $\mathcal{G}^\mu$ and f, it is straightforward to verify that A and $\widehat{A}$ are linear and continuous operators in g such that $A(0;\mu) \equiv 0$, and $\widehat{A}(0;\mu) \equiv 0$. Finally, we introduce the manifolds

$$\widehat{A}(\mathcal{T}) := \{u_g(\mu) : \ \mu \in \mathcal{P},\ g \in \mathcal{T}\} \subset \mathcal{V}, \tag{3a}$$

and

$$A(\mathcal{T}) := \{u_g(\mu)|_\Omega : \ \mu \in \mathcal{P},\ g \in \mathcal{T}\} \subset \mathcal{Y}. \tag{3b}$$

In the remainder of this section, we discuss the data compression strategy for the construction of a linear approximation space $\mathcal{Z}_N$ for the manifold $A(\mathcal{T})$. First, we consider the case $\mathcal{P} = \{\bar{\mu}\}$, and then we consider the extension to the general case $\mathcal{P} \neq \{\bar{\mu}\}$. In the case $\mathcal{P} = \{\bar{\mu}\}$, to simplify notation, we omit the dependence on the parameter.

2.2. The case $\mathcal{P} = \{\bar{\mu}\}$. We introduce the *transfer eigenproblem* as follows: find $(\phi_n, \lambda_n) \in (\mathcal{T}, \mathbb{R}_+)$ such that

$$(A(\phi_n),\, A(g))_{\mathcal{Y}} \;=\; \lambda_n (\phi_n,\, g)_{\mathcal{T}} \qquad \forall\, g \in \mathcal{T}, \tag{4}$$

where $\lambda_1 \geq \lambda_2 \ldots \geq 0$ and $(\phi_n, \phi_{n'})_{\mathcal{T}} = \delta_{n,n'}$. Then, for any $N > 0$, we define the *transfer eigenspace*

$$\mathcal{Z}_N^{\rm te} := \mathrm{span}\{A(\phi_n)\}_{n=1}^N. \tag{5}$$

If we introduce the finite-dimensional discretization of $\mathcal{T}$, $\mathcal{T}_{\mathcal{N}_{\rm in}} = \mathrm{span}\{g_1, \ldots, g_{\mathcal{N}_{\rm in}}\} \subset \mathcal{T}$, we can define the semi-discrete transfer eigenproblem: find $(\phi_n^{\mathcal{N}_{\rm in}}, \lambda_n^{\mathcal{N}_{\rm in}}) \in (\mathcal{T}_{\mathcal{N}_{\rm in}}, \mathbb{R}_+)$ such that

$$(A(\phi_n^{\mathcal{N}_{\rm in}}),\, A(g))_{\mathcal{Y}} \;=\; \lambda_n^{\mathcal{N}_{\rm in}} (\phi_n^{\mathcal{N}_{\rm in}},\, g)_{\mathcal{T}} \qquad \forall\, g \in \mathcal{T}_{\mathcal{N}_{\rm in}}, \tag{6}$$

where $\lambda_1^{\mathcal{N}_{\rm in}} \geq \lambda_2^{\mathcal{N}_{\rm in}} \ldots \geq \lambda_{\mathcal{N}_{\rm in}}^{\mathcal{N}_{\rm in}} \geq 0$, and $(\phi_n^{\mathcal{N}_{\rm in}}, \phi_{n'}^{\mathcal{N}_{\rm in}})_{\mathcal{T}} = \delta_{n,n'}$. Then, for any $N > 0$, we define the semi-discrete transfer eigenspace:

$$\mathcal{Z}_N^{{\rm te},\mathcal{N}_{\rm in}} := {\rm span}\{A(\phi_n^{\mathcal{N}_{\rm in}})\}_{n=1}^N. \tag{7}$$

Eigenproblem (6) can also be restated in a fully algebraic form as

$$\mathbb{U}\,\boldsymbol{\phi}_n^{\mathcal{N}_{\rm in}} = \lambda_n^{\mathcal{N}_{\rm in}} \mathbb{T} \boldsymbol{\phi}_n^{\mathcal{N}_{\rm in}}, \qquad \text{for } n = 1, \ldots, \mathcal{N}_{\rm in}, \tag{8a}$$

where $\mathbb{U}, \mathbb{T} \in \mathbb{R}^{\mathcal{N}_{\rm in},\mathcal{N}_{\rm in}}$ are given by

$$\mathbb{U}_{i,i'} = (A(g_i), A(g_{i'}))_{\mathcal{Y}}, \quad \mathbb{T}_{i,i'} = (g_i, g_{i'})_{\mathcal{T}}, \quad i, i' = 1, \ldots, \mathcal{N}_{\rm in}, \tag{8b}$$

and the vectors $\{\boldsymbol{\phi}_n^{\mathcal{N}_{\rm in}}\}_n$ are related to the transfer eigenmodes $\{\phi_n^{\mathcal{N}_{\rm in}}\}_n$ by the relation

$$\phi_n^{\mathcal{N}_{\rm in}} = \sum_{i=1}^{\mathcal{N}_{\rm in}} (\boldsymbol{\phi}_n^{\mathcal{N}_{\rm in}})_i \, g_i. \tag{8c}$$

We observe that eigenproblem (8) is not fully actionable since evaluations of the map $A(\cdot)$ involve the solution to a PDE: we should thus replace A with the corresponding Finite Element (FE) counterpart $A^{\rm FE}$. To simplify notation, we here omit the superscript $^{\rm FE}$.

The transfer eigenproblem is tightly connected to the eigenproblem obtained using POD. In more detail, if we choose an orthonormal basis $\{g_n\}_{n=1}^{\mathcal{N}_{\rm in}}$ for $\mathcal{T}_{\mathcal{N}_{\rm in}}$, (8) reduces to the eigenproblem

$$\mathbb{U}\,\boldsymbol{\phi}_n^{\mathcal{N}_{\rm in}} = \lambda_n^{\mathcal{N}_{\rm in}} \boldsymbol{\phi}_n^{\mathcal{N}_{\rm in}}, \qquad \text{for } n = 1, \ldots, \mathcal{N}_{\rm in};$$

this corresponds to the eigenproblem obtained by applying POD based on the method of snapshots ([33]) to the set $\{A(g_n)\}_{n=1}^{\mathcal{N}_{\rm in}}$. We observe that, unlike the reduced space generated by POD[1], the reduced space $\mathcal{Z}_N^{{\rm te},\mathcal{N}_{\rm in}}$ is independent of the particular basis of $\mathcal{T}_{\mathcal{N}_{\rm in}}$ employed.

The connection between transfer eigenproblem and POD can also be established in terms of SVD. It is indeed possible to show that the transfer eigenproblem computes the truncated SVD of the operator A, whereas POD computes the truncated SVD of the operator which maps the n-th canonical basis vector of $\mathbb{R}^{\mathcal{N}_{\rm in}}$ to $A(g_n)$ for a given basis $\{g_n\}_{n=1}^{\mathcal{N}_{\rm in}}$. The choice of an orthonormal basis $\{g_n\}_{n=1}^{\mathcal{N}_{\rm in}}$ induces an isometry between $\mathbb{R}^{\mathcal{N}_{\rm in}}$ and $\mathcal{T}_{\mathcal{N}_{\rm in}}$. Hence, both operators have the same left-singular vectors.

2.3. The case $\mathcal{P} \neq \{\bar{\mu}\}$. If $\mathcal{P} \neq \{\bar{\mu}\}$, we adopt a two-stage procedure based on the combination of the method presented above and POD. We first consider a finite-dimensional discretization of $\mathcal{P}$, $\mathcal{P}_{\rm train} = \{\mu^i\}_{i=1}^{n_{\rm train}}$. Then, we solve $n_{\rm train}$ transfer eigenproblems, one for each value of the parameter, to obtain $n_{\rm train}$ N-dimensional transfer eigenspaces $\{\mathcal{Z}_N^{{\rm te},\mathcal{N}_{\rm in}}(\mu^i)\}_{i=1}^{n_{\rm train}}$. Finally, we generate the background space $\mathcal{Z}_N$ by applying POD — based on the $\mathcal{Y}$ inner product — to the set of snapshots $\{A(\phi_n^{\mathcal{N}_{\rm in},i}; \mu^i)\}_{i,n}$, where $\|\phi_n^{\mathcal{N}_{\rm in},i}\|_{\mathcal{T}} = 1$ for all $i = 1, \ldots, n_{\rm train}$ and $n = 1, \ldots, N$. Algorithm 1 summarises the computational procedure.

[1] More precisely, the POD space and the POD eigenvalues associated with $\{A(g_n)\}_n$ are the same for any orthonormal basis of $\mathcal{T}_{\mathcal{N}_{\rm in}}$. On the other hand, POD space and eigenvalues might vary for different non-orthonormal bases of $\mathcal{T}_{\mathcal{N}_{\rm in}}$.

Algorithm 1 Construction of the localized reduced space

Input	$\mathcal{P}_{\text{train}} = \{\mu^i\}_{i=1}^{n_{\text{train}}} \subset \mathcal{P}$	discretized parameter space
	N	dimension of the background space
Output	$\mathcal{Z}_N$	background space

1: Define the basis $\{g_1, \ldots, g_{\mathcal{N}_{\text{in}}}\}$ for $\mathcal{T}_{\mathcal{N}_{\text{in}}}$.

2: **for** $i = 1 \ldots n_{\text{train}}$ **do**

3: Compute the first N normalized eigenmodes $\{\phi_n^{\mathcal{N}_{\text{in}},i}\}_{n=1}^N$ associated with $A^i := A(\cdot;\mu^i)$ using (6), ($\|\phi_n^{\mathcal{N}_{\text{in}},i}\|_{\mathcal{T}} = 1$, $i = 1, \ldots, n_{\text{train}}$, $n = 1, \ldots, N$).

4: **end for**

5: Apply POD to the set of snapshots $\{A(\phi_n^{\mathcal{N}_{\text{in}},i};\mu^i)\}_{i=1,\ldots,n_{\text{train}},\, n=1,\ldots,N}$ to generate $\mathcal{Z}_N \subset \mathcal{Y}$.

We observe that

$$\|A(\phi_n^{\mathcal{N}_{\text{in}},i};\mu^i)\|_{\mathcal{Y}}^2 \;=\; (A(\phi_n^{\mathcal{N}_{\text{in}},i};\mu^i),\, A(\phi_n^{\mathcal{N}_{\text{in}},i};\mu^i)) = \lambda_n^{\mathcal{N}_{\text{in}},i}\,(\phi_n^{\mathcal{N}_{\text{in}},i},\, \phi_n^{\mathcal{N}_{\text{in}},i})_{\mathcal{T}} \;=\; \lambda_n^{\mathcal{N}_{\text{in}},i}.$$

Therefore, the POD reduction implicitly takes into account the relative importance — quantified by the value of the corresponding transfer eigenvalue — of the different snapshots. Exploiting the relationship between POD modes and transfer eigenmodes explained in the previous section, we can interpret Algorithm 1 as a distributed approximated POD ([17]) based on two layers: the first layer addresses the uncertainty in the boundary conditions, the second layer addresses the parameter variation. We further observe that we could keep $\widetilde{N} > N$ POD modes: if parameter variation is significant, we anticipate that $\lambda_N^{\text{POD}} \gg \max_i \lambda_N^{\mathcal{N}_{\text{in}},i}$ where λ_N^{POD} denotes the N-th POD eigenvalue; for this reason, we could select N based on $\{\lambda_n^{\mathcal{N}_{\text{in}},i}\}_{i,n}$, and then $\widetilde{N}$ based on $\{\lambda_n^{\text{POD}}\}_n$. Finally, we observe that the construction of $\mathcal{Z}_N$ requires the solution to $n_{\text{train}} \times \mathcal{N}_{\text{in}}$ PDEs in the bk domain Ω^{bk}, the solution to n_{train} eigenproblems of size $\mathcal{N}_{\text{in}}$, and the solution to an eigenproblem of size $n_{\text{train}} \times N$. Although the computations can be trivially parallelized, we envision that Algorithm 1 is affordable only for moderate values of n_{train}. Therefore, our technique can be applied only to low-dimensional parameter spaces $\mathcal{P}$. The latter of course does not include any parameters outside Ω^{bk} (i.e., in $\Omega^{\text{pb}} \setminus \Omega^{\text{bk}}$).

In [34], a different strategy to construct $\mathcal{Z}_N$ for non-trivial parameter spaces is presented. Rather than performing a POD (cf. step 5 Algorithm 1), in [34] the authors propose a Greedy algorithm that iteratively augments the space $\mathcal{Z}_N$ with the transfer eigenspaces generated for a single value of the parameter. Both approaches require the solution to the same number of transfer eigenproblems, and thus the same number of PDE solves (equal to $n_{\text{train}} \times \mathcal{N}_{\text{in}}$): since the solution to the n_{train} transfer eigenproblems is by far the most demanding step of both procedures, the two approaches are nearly equivalent in terms of overall computational cost. The POD reduction proposed here is easier to implement compared to the approach in [34]; on the other hand, we envision that a comparison of the performance of the two methods is extremely problem-dependent.

3. Analysis.

3.1. Optimal approximation spaces. In view of the analysis, we present a first definition of optimality in the sense of Kolmogorov ([27]).

DEFINITION 3.1. *Given $N > 0$, and $A : \mathcal{T} \to \mathcal{Y}$, we say that $Z_N^{\text{kolm}} \subset \mathcal{Y}$ is an optimal N-dimensional approximation space for $A(\mathcal{T}) := \{A(g) : g \in \mathcal{T}\}$ if and only if*

$$Z_N^{\text{kolm}} \in \arg \inf_{Z_N \subset \mathcal{Y},\, \dim Z_N = N} d\left(A(\mathcal{T}), Z_N\right), \tag{9a}$$

where $d\left(A(\mathcal{T}), Z_N\right)$ is defined as

$$d\left(A(\mathcal{T}), Z_N\right) = \sup_{g \in \mathcal{T}, \|g\|_{\mathcal{T}} \neq 0} \frac{\|A(g) - \Pi_{Z_N}^{\mathcal{Y}} A(g)\|_{\mathcal{Y}}}{\|g\|_{\mathcal{T}}}. \tag{9b}$$

We say that $d_N(A(\mathcal{T})) = d\left(\mathcal{A}(\mathcal{T}), Z_N^{\text{kolm}}\right)$ is the Kolmogorov N-width associated with the manifold $A(\mathcal{T})$.

Several variants of Kolmogorov N-width have been proposed in the literature. In the MOR literature, given the compact manifold $\mathcal{M} \subset \mathcal{Y}$, Kolmogorov N-width is defined as (see, e.g., [9])

$$\bar{d}_N(\mathcal{M}) = \inf_{Z_N \subset \mathcal{Y},\, \dim Z_N = N} \sup_{u \in \mathcal{M}} \|u - \Pi_{Z_N}^{\mathcal{Y}} u\|_{\mathcal{Y}}. \tag{10}$$

In Appendix A, we rigorously relate (9b) to (10) for a proper choice of $\mathcal{M} \subset A(\mathcal{T})$ (cf. Proposition A.1).

Kolmogorov N-widths measure the performance of the best linear approximation space of size N: they thus provide a lower bound for the best-fit error associated with any N-dimensional linear space obtained using a model-reduction technique. For this reason, we can interpret Kolmogorov N-widths as measures of the reducibility of the manifold $\mathcal{M}$. *A priori* results for the convergence of the N-width with N are available for several classes of problems: see [14, Example 3.4], [31, Section 8.1.1], [37, Example 2.5], [2, Theorem 3.3], and [10]. Several empirical studies suggest that N-widths converge rapidly for diffusion-dominated problems, and significantly less rapidly for advection-dominated problems; as discussed in [36, Chapter 5.1.2], this is strongly related to the concept of evanescence.

We now provide another definition of optimality. For simplicity, we state the definition for a finite set of snapshots rather than a continuous manifold. We refer to [3, section 2.3] and to [38, section 1.3] for the generalization of this definition to continuous manifolds.

DEFINITION 3.2. *Given $N > 0$, and the set of snapshots $\mathcal{S} = \{u_i\}_{i=1}^{|\mathcal{S}|}$, we say that $Z_N^{\ell^2} \subset \mathcal{Y}$ is an optimal N-dimensional approximation space for $\mathcal{S}$ in the ℓ^2-sense if and only if*

$$Z_N^{\ell^2} \in \arg \inf_{Z_N \subset \mathcal{Y},\, \dim Z_N = N} d^{\ell^2}(\mathcal{S}, Z_N) := \frac{1}{|\mathcal{S}|} \sum_{i=1}^{|\mathcal{S}|} \|u_i - \Pi_{Z_N}^{\mathcal{Y}} u_i\|_{\mathcal{Y}}^2. \tag{11}$$

We further define $d_N^{\ell^2}(\mathcal{S}) := d^{\ell^2}(\mathcal{S}, Z_N^{\ell^2})$

3.2. The case $\mathcal{P} = \{\bar{\mu}\}$. We first state the key result of this section. We refer to [27, Chapter 4, Theorem 2.2] for the proof. As in section 2.2, we omit the dependence on the parameter $\bar{\mu}$.

PROPOSITION 3.3. *Let $A : \mathcal{T} \to \mathcal{Y}$ defined in (2) be a linear compact operator. Then, for any $N > 0$ the space $\mathcal{Z}_N^{\text{te}}$ defined in (5) is an optimal N-dimensional approximation space for $A(\mathcal{T})$. Furthermore,*

$$d(A(\mathcal{T})) = \sqrt{\lambda_{N+1}}. \tag{12}$$

REMARK 3.4. ***(sufficient conditions for compactness)*** *Proposition 3.3 shows that the reduced space built by solving the transfer eigenproblem is optimal in the sense of Kolmogorov if the solution map A (2) is compact. Given a particular bk model, we should thus assess whether the corresponding solution map A is compact. In Appendix A, (cf. Proposition A.2), we provide sufficient conditions — which are satisfied by the examples considered in this paper — under which the solution map associated with a given mathematical model is compact.*

The next Proposition provides an upper bound on the performance of the semi-discrete transfer eigenspace $Z_N^{\text{te},\mathcal{N}_{\text{in}}}$ (7).

PROPOSITION 3.5. *Let $\mathcal{T}_{\mathcal{N}_{\text{in}}} = \text{span}\{g_1, \dots, g_{\mathcal{N}_{\text{in}}}\} \subset \mathcal{T}$, and let $\mathcal{Z}_N^{\text{te},\mathcal{N}_{\text{in}}}$ be the corresponding semi-discrete transfer eigenspace (7) computed based on (8). For any $g \in \mathcal{T}$, we have*

$$\frac{\|A(g) - \Pi^{\mathcal{Y}}_{\mathcal{Z}_N^{\text{te},\mathcal{N}_{\text{in}}}} A(g)\|_{\mathcal{Y}}}{\|g\|_{\mathcal{T}}} \leq \|A\|_{\mathcal{L}(\mathcal{T}^{\perp}_{\mathcal{N}_{\text{in}}},\mathcal{Y})} \frac{\|\Pi^{\mathcal{T}}_{\mathcal{T}^{\perp}_{\mathcal{N}_{\text{in}}}} g\|_{\mathcal{T}}}{\|g\|_{\mathcal{T}}} + \sqrt{\lambda^{\mathcal{N}_{\text{in}}}_{N+1}}, \tag{13}$$

where $\lambda^{\mathcal{N}_{\text{in}}}_{N+1}$ is the $N+1$ eigenvalue of the semi-discrete eigenproblem (6).

Proof. Exploiting the linearity of the operator A and applying (12) in the finite dimensional case, we find

$$\begin{aligned}
&\inf_{\phi \in \mathcal{Z}_N^{\text{te},\mathcal{N}_{\text{in}}}} \|A(g) - \phi\|_{\mathcal{Y}} \\
&\qquad \leq \inf_{\phi \in \mathcal{Z}_N^{\text{te},\mathcal{N}_{\text{in}}}} \|A(g) - A\left(\Pi^{\mathcal{T}}_{\mathcal{T}_{\mathcal{N}_{\text{in}}}} g\right)\|_{\mathcal{Y}} + \|A\left(\Pi^{\mathcal{T}}_{\mathcal{T}_{\mathcal{N}_{\text{in}}}} g\right) - \phi\|_{\mathcal{Y}} \\
&\qquad \leq \|A\|_{\mathcal{L}(\mathcal{T}^{\perp}_{\mathcal{N}_{\text{in}}},\mathcal{Y})} \|\Pi^{\mathcal{T}}_{\mathcal{T}^{\perp}_{\mathcal{N}_{\text{in}}}} g\|_{\mathcal{T}} + \inf_{\phi \in \mathcal{Z}_N^{\text{te},\mathcal{N}_{\text{in}}}} \|A\left(\Pi^{\mathcal{T}}_{\mathcal{T}_{\mathcal{N}_{\text{in}}}} g\right) - \phi\|_{\mathcal{Y}} \\
&\qquad \leq \|A\|_{\mathcal{L}(\mathcal{T}^{\perp}_{\mathcal{N}_{\text{in}}},\mathcal{Y})} \|\Pi^{\mathcal{T}}_{\mathcal{T}^{\perp}_{\mathcal{N}_{\text{in}}}} g\|_{\mathcal{T}} + \underbrace{d(A(\mathcal{T}_{\mathcal{N}_{\text{in}}}), \mathcal{Z}_N^{\text{te},\mathcal{N}_{\text{in}}})}_{=\sqrt{\lambda^{\mathcal{N}_{\text{in}}}_{N+1}}} \|g\|_{\mathcal{T}},
\end{aligned}$$

Thesis follows. ∎

Exploiting (13), we observe that the best-fit error $\|A(g) - \Pi^{\mathcal{Y}}_{\mathcal{Z}_N^{\text{te},\mathcal{N}_{\text{in}}}} A(g)\|_{\mathcal{Y}}$ is controlled by the sum of two contributions: the former — $\|A\|_{\mathcal{L}(\mathcal{T}^{\perp}_{\mathcal{N}_{\text{in}}},\mathcal{Y})} \|\Pi^{\mathcal{T}}_{\mathcal{T}^{\perp}_{\mathcal{N}_{\text{in}}}} g\|_{\mathcal{T}}$ — takes into account errors in the choice of $\mathcal{T}_{\mathcal{N}_{\text{in}}}$; the latter — $\sqrt{\lambda^{\mathcal{N}_{\text{in}}}_{N+1}}\|g\|_{\mathcal{T}}$— takes into account the error associated with the truncation of the transfer eigen-expansion. The first contribution in (13) shows the robustness of our approach to errors in the choice of $\mathcal{T}_{\mathcal{N}_{\text{in}}}$. In this respect, we observe that the discretization error associated with the input space is multiplied the operator norm A over $\mathcal{T}^{\perp}_{\mathcal{N}_{\text{in}}}$, $\|A\|_{\mathcal{L}(\mathcal{T}^{\perp}_{\mathcal{N}_{\text{in}}},\mathcal{Y})}$. By exploiting a separation-of-variable argument (see [34, Remark 3.6]), we expect

that for several relevant applications[2] highly-oscillatory modes on Γ^{in} decay fast in the interior of the domain Ω^{bk}. Therefore, if we choose a smooth input space (e.g., the space of polynomials of degree less than $\mathcal{N}_{\text{in}}$), the operator norm $\|A\|_{\mathcal{L}(\mathcal{T}_{\mathcal{N}_{\text{in}}}^{\perp},\mathcal{Y})}$ should decay rapidly with $\mathcal{N}_{\text{in}}$. This implies that even fields that have low regularity on Γ^{in} can be well-approximated by the transfer eigenspace; in section 4.3, we present numerical evidence that supports our claim.

The robustness of the approach to discretization error on Γ^{in} is important in the context of data assimilation: in many engineering applications, the set of possible inputs might be very high-dimensional, but it might be well-approximated by a lower dimensional space. Proposition 3.5 shows that we can reduce the dimension of the discrete input space without significantly deteriorating the approximation properties of $\mathcal{Z}_N^{\text{te},\mathcal{N}_{\text{in}}}$.

We conclude this section with a remark.

REMARK 3.6. *(**Optimality in the** ℓ^2 **sense**) Let $\{\psi_n\}_{n=1}^{\mathcal{N}_{\text{in}}}$ be an orthonormal basis of $\mathcal{T}_{\mathcal{N}_{\text{in}}}$. Then, exploiting the connection between transfer eigenmodes and POD eigenmodes shown in section 2, we have that*

$$\mathcal{Z}_N^{\text{te},\mathcal{N}_{\text{in}}} \in \arg \inf_{Z_N \subset \mathcal{Y},\, \dim Z_N = N} d^{\ell^2}(\mathcal{S}, Z_N), \tag{14}$$

where $\mathcal{S} = \{A(\psi_n)\}_{n=1}^{\mathcal{N}_{\text{in}}}$ and d^{ℓ^2} is defined in (11). We observe that (14) holds for any orthonormal basis of $\mathcal{T}_{\mathcal{N}_{\text{in}}}$.

3.3. The case $\mathcal{P} \neq \{\bar{\mu}\}$. Exploiting the connection with Hierarchical Approximate Proper Orthogonal Decomposition, we can show the following Proposition.

PROPOSITION 3.7. *Let $\{g_1, \dots, g_{\mathcal{N}_{\text{in}}}\} \subset \mathcal{T}$ be an orthonormal basis of $\mathcal{T}_{\mathcal{N}_{\text{in}}}$. Let us define $\epsilon_N^{\text{te,i}} = \sum_{n=N+1}^{\mathcal{N}_{\text{in}}} \lambda_n^{\mathcal{N}_{\text{in}},i}$ for $i = 1, \dots, n_{\text{train}}$, where $\{\lambda_n^{\mathcal{N}_{\text{in}},i}\}_{n=1}^{\mathcal{N}_{\text{in}}}$ are the transfer eigenvalues associated with (6). Let us further define $\epsilon_N^{\text{POD}} = \sum_{n=N+1}^{N n_{\text{train}}} \lambda_n^{\text{POD}}$, where $\{\lambda_n^{\text{POD}}\}_{n=1}^{N n_{\text{train}}}$ are the POD eigenvalues. Then, the following bound holds:*

$$\frac{1}{\mathcal{N}_{\text{in}} n_{\text{train}}} \sum_{n=1}^{\mathcal{N}_{\text{in}}} \sum_{i=1}^{n_{\text{train}}} \|A(g_n;\mu^i) - \Pi_{\mathcal{Z}_N}^{\mathcal{Y}} A(g_n;\mu^i)\|_{\mathcal{Y}}^2 \leq \left(\epsilon^{\text{te,pod}}\right)^2, \tag{15a}$$

where $\epsilon^{\text{te,pod}}$ is given by

$$\epsilon^{\text{te,pod}} = \frac{1}{\sqrt{\mathcal{N}_{\text{in}} n_{\text{train}}}} \sqrt{n_{\text{train}} \max_i \epsilon_N^{\text{te,i}} + \epsilon_N^{\text{POD}}}. \tag{15b}$$

Furthermore, the number of POD modes associated with $\{A(g_n;\mu^i)\}_{i,n}$ required to obtain the accuracy $\tilde{\epsilon}^2 = \frac{\epsilon_N^{\text{POD}}}{n_{\text{train}} \cdot \mathcal{N}_{\text{in}}}$ is greater or equal than N:

$$N \leq \min\left\{N' \in \{1, \dots, n_{\text{train}} \cdot \mathcal{N}_{\text{in}}\} : \; d_{N'}^{\ell^2}(\{A(g_n;\mu^i)\}_{n,i}) \leq \tilde{\epsilon}^2\right\}, \tag{15c}$$

where $d_N^{\ell^2}$ is introduced in Definition 3.2.

[2] As for the decay of the Kolmogorov N-width discussed in the introduction, the behavior of $\|A\|_{\mathcal{L}(\mathcal{T}_{\mathcal{N}_{\text{in}}}^{\perp},\mathcal{Y})}$ with $\mathcal{N}_{\text{in}}$ is an intrinsic feature of the problem considered, and should thus be assessed on a case-by-case basis.

Proof. As observed in section 2.3, our algorithm corresponds to a distributed approximate POD. Applying [17, Theorem 3.5], we find

$$\frac{1}{\mathcal{N}_{\text{in}} n_{\text{train}}} \sum_{n=1}^{\mathcal{N}_{\text{in}}} \sum_{i=1}^{n_{\text{train}}} \|A(g_n;\mu^i) - \Pi^{\mathcal{Y}}_{\mathcal{Z}_N} A(g_n;\mu^i)\|^2_{\mathcal{Y}} \leq \inf_{\omega\in(0,1)} (\epsilon^{\text{te,pod}}(\omega))^2,$$

where $\epsilon^{\text{te,pod}}(\omega)$ is given by

$$\epsilon^{\text{te,pod}}(\omega) = \frac{1}{\sqrt{\mathcal{N}_{\text{in}} n_{\text{train}}}} \max\left\{ \sqrt{\frac{n_{\text{train}}}{1-\omega^2} \max_i \epsilon^{\text{te,i}}_N},\ \sqrt{\frac{\epsilon^{\text{POD}}_N}{\omega^2}} \right\},\quad \omega \in (0,1).$$

Thesis then follows by minimizing $\epsilon^{\text{te,pod}}(\omega)$ with respect to ω. Table 1 clarifies the link between the definitions appearing in [17, Theorem 3.5] and the corresponding definitions of Proposition 3.7.

[17, Theorem 3.5]	explanation	Prop. 3.7
$\epsilon_{\mathcal{T}}(\rho_{\mathcal{T}})$	tolerance for the POD reduction step	$\sqrt{\epsilon^{\text{POD}}_N}$
$L_{\mathcal{T}}$	number of reduction stages	2
$\lvert\mathcal{S}\rvert$	cardinality of the snapshot set	$\mathcal{N}_{\text{in}} \times n_{\text{train}}$
$\lvert\widetilde{\mathcal{S}}_\alpha\rvert$	cardinality of the snapshot set for a given μ	$\mathcal{N}_{\text{in}}$
$\epsilon_{\mathcal{T}}(\alpha)$	tolerance for the transfer eigenproblem	$\sqrt{\epsilon^{\text{te},\alpha}_N}$

Table 1: explanation of the link between notation of [17, Theorem 3.5] and notation of Proposition 3.7.

Proposition 3.7 is a suboptimal result. Estimate (15c) fixes a lower bound for the number of POD modes required to obtain the same accuracy in a ℓ^2 sense. We remark that in order to apply a global POD we must assemble a full matrix of size $n_{\text{train}} \times \mathcal{N}_{\text{in}}$; this might be unfeasible for practical applications. We observe that $\epsilon^{\text{POD}}_N \simeq \max_i \epsilon^{\text{te,i}}_N$ implies redundancy between different values of μ; on the other hand, $\epsilon^{\text{POD}}_N \gg \max_i \epsilon^{\text{te,i}}_N$ corresponds to the scenario in which parameter variation has a major contribution in determining the final reduced space. Finally, we observe that the proof does not exploit the optimality of the transfer eigenspace (cf. Proposition 3.3) for fixed μ. For this reason, we envision that the result might be improved in our particular setting.

4. Application to state estimation.

4.1. An acoustic model problem. We illustrate the application of our localization procedure to state estimation. Towards this end, we introduce the following model problem:

$$\begin{cases} -(1+\texttt{i}\epsilon)\Delta u^{\text{true}}(\mu) - \mu^2 u^{\text{true}}(\mu) = f & \text{in } \Omega^{\text{pb}}; \\ \partial_n u^{\text{true}}(\mu) = 0 & \text{on } \partial\Omega^{\text{pb}} \setminus \Gamma; \\ u^{\text{true}}(\mu) = h^{\text{true}} & \text{on } \Gamma; \end{cases} \tag{16}$$

where $\Gamma \subset \partial\Omega^{\rm pb}$ is an open set, $\mathtt{i} = \sqrt{-1}$ is the imaginary unit, $\epsilon = 10^{-4}$, $f(x) = 10\mathbb{1}_{[-0.5,0]}(x_1)\mathbb{1}_{[1.25,1.75]}(x_2)$. The function f can be interpreted as an acoustic volumetric source associated with a speaker placed outside $\Omega^{\rm bk}$. In our numerical simulations, we consider $h^{\rm true} = h_k(x_2) = \sin(\pi k x_2)$ for $k = 1, 2, 3$, we consider several choices of μ in $\mathcal{P} = [2, 4]$, and we consider two different choices of the problem domain $\Omega^{\rm pb}$, $\Omega^{\rm pb,1}$ and $\Omega^{\rm pb,2}$, which are depicted in Figure 2. In this example, $h^{\rm true}$, $\Omega^{\rm pb}$ and f represent parameters outside our control, while we assume that μ belongs to the confidence region $\mathcal{P}$: the uncertainty in the value of μ represents the parametric uncertainty in the system. We then introduce the domain of interest $\Omega = (2, 3)^2$, the bk domain $\Omega^{\rm bk} = (0, 3)^2$, and the bk model:

$$
\begin{cases}
-(1+\epsilon\mathtt{i})\Delta u_g(\mu) - \mu^2 u_g(\mu) = 0 & \text{in } \Omega^{\rm bk};\\
\partial_n u_g(\mu) = 0 & \text{on } \partial\Omega^{\rm bk} \setminus \Gamma^{\rm in};\\
u_g(\mu) = g & \text{on } \Gamma^{\rm in};
\end{cases}
\tag{17}
$$

where $\Gamma^{\rm in} = \{0\} \times (0, 3)$. We remark that $\Omega, \Omega^{\rm bk}$, $\Gamma^{\rm in}$, and the bk model are the same for both choices of the problem domain $\Omega^{\rm pb}$. If we denote by A the local bk solution operator, since $f|_{\Omega^{\rm bk}} \equiv 0$, we find that $u^{\rm true}(\mu)|_\Omega = A(u^{\rm true}(\mu)|_{\Gamma^{\rm in}}, \mu)$; therefore, $u^{\rm true}(\mu)|_\Omega \in A(\mathcal{T}) := \{u_g|_\Omega : \mu \in \mathcal{P}, g \in \mathcal{T} = H^{1/2}(\Gamma^{\rm in})\}$ for any $h^{\rm true} \in H^{1/2}(\Gamma)$, for any $\mu \in \mathcal{P}$, and for both choices of $\Omega^{\rm pb}$ in (16).

Our goal is to estimate the acoustic field $u^{\rm true}$ in the domain Ω based on M measurements of the form

$$
\ell_m^{\rm obs} = \ell(u^{\rm true}; x_m^{\rm obs}, r_{\rm Gauss}) := C(x_m^{\rm obs}) \int_\Omega u^{\rm true}(y) \exp\left(-\frac{|y - x_m^{\rm obs}|^2}{2r_{\rm Gauss}^2}\right) dy,
\tag{18}
$$

and on the knowledge of the bk model (17). The constant C is chosen such that $\ell(1; x, r_{\rm Gauss}) \equiv 1$ for all $x \in \Omega$, the parameter $r_{\rm Gauss}$ is set equal to 0.1, while the choice of the observation centers $\{x_m^{\rm obs}\}_{m=1}^M$ is discussed in the next section. The functional ℓ mimics the local average of the acoustic pressure as might be measured by a physical transducer (see [21]).

We briefly motivate our model problem. As discussed in the introduction, for practical problems, it might be difficult to develop a parametrized model for the full system in $\Omega^{\rm pb}$. Provided that the uncertainty associated with the shape of $\Omega^{\rm pb}$ is confined to $\Omega^{\rm pb} \setminus \Omega^{\rm bk}$, and that the support of f is outside $\Omega^{\rm bk}$, the uncertainty in $\Omega^{\rm pb}$ and f (and $h^{\rm true}$) can be fully addressed through the boundary condition on $\Gamma^{\rm in}$. This demonstrates that localization significantly simplifies the parametrization of the problem. Furthermore, since $\Gamma^{\rm in}$ is sufficiently far from Ω, we can exploit the procedure developed in this paper to obtain a low-dimensional reduced space for $A(\mathcal{T})$, which will be accurate for the original system regardless of the shape of $\Omega^{\rm pb}$ and of the precise form of the source f. Therefore, localization also leads to significant uncertainty reduction. We numerically confirm these observations in the next sections.

Computations are based on a P4 FE discretization with $\mathcal{N}^{\rm pb} = 12289$ ($\mathcal{N}^{\rm pb} = 11825$) degrees of freedom in $\Omega^{\rm pb,1}$ ($\Omega^{\rm pb,2}$), $\mathcal{N}^{\rm bk} = 9409$ degrees of freedom in $\Omega^{\rm bk}$, and $\mathcal{N} = 1089$ degrees of freedom in Ω. Figures 3 and 4 show the field $u^{\rm true}(\mu)$ for different $h^{\rm true}$ and μ, and for the two problem domains $\Omega^{\rm pb,1}, \Omega^{\rm pb,2}$. Figure 5 shows the variations in $\|u^{\rm true}(\mu)\|_{H^1(\Omega^{\rm pb})}$ as a function of μ for $h^{\rm true} = h_1$; note that there are ten resonances for $\Omega^{\rm pb,1}$ and eleven resonances for $\Omega^{\rm pb,2}$ in the parameter range $\mathcal{P} = [2, 4]$.

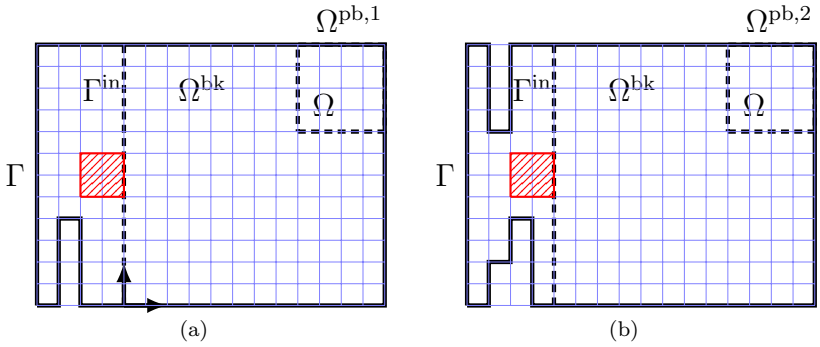

Fig. 2: Application to state estimation: geometry. The filled region indicates the support of the source f. The edges of the squares of the grid are of length 0.25.

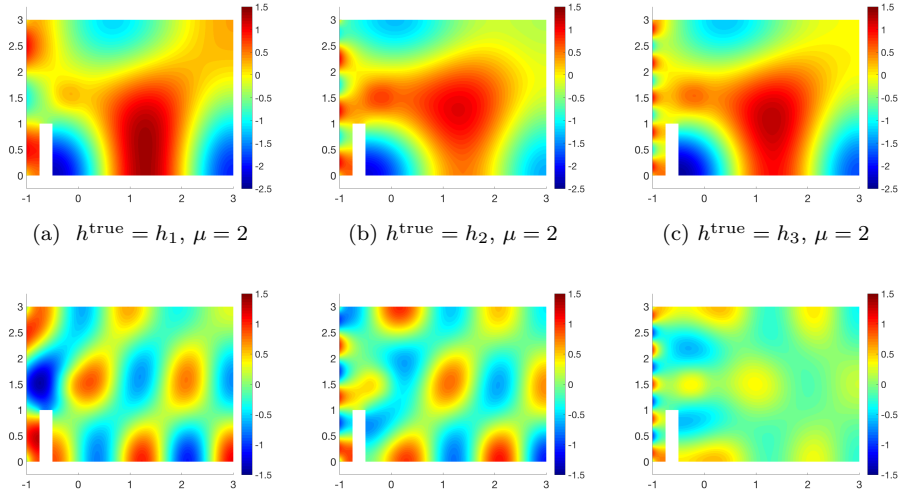

(a) $h^{\text{true}} = h_1$, $\mu = 2$ (b) $h^{\text{true}} = h_2$, $\mu = 2$ (c) $h^{\text{true}} = h_3$, $\mu = 2$

(d) $h^{\text{true}} = h_1$, $\mu = 4$ (e) $h^{\text{true}} = h_2$, $\mu = 4$ (f) $h^{\text{true}} = h_3$, $\mu = 4$

Fig. 3: Application to state estimation: visualization of the real part of the true field $\text{Re}\{u^{\text{true}}(\mu)\}$ for $\Omega^{\text{pb},1}$.

4.2. Formulation: the PBDW approach. Given the measurements $\{\ell_m^{\text{obs}} = \ell_m^o(u^{\text{true}})\}_{m=1}^M \subset \mathbb{C}$, and the N-dimensional *background space* $\mathcal{Z}_N \subset \mathcal{Y} := H^1(\Omega)$, we define the PBDW state estimate $u^\star = z^\star + \eta^\star$ as the solution to the following minimization statement ([21, 22, 35]):

$$\min_{(z,\eta)\in\mathcal{Z}_N\times\mathcal{Y}} \|\eta\|_{\mathcal{Y}}, \quad \text{subject to } \ell_m^o(z+\eta) = \ell_m^{\text{obs}}, \ \ m = 1,\dots,M; \tag{19}$$

where $\|\cdot\|_{\mathcal{Y}} = \sqrt{(\cdot,\cdot)_{\mathcal{Y}}}$, $(u,v)_{\mathcal{Y}} = \int_\Omega \nabla u\cdot\nabla\bar{v} + u\bar{v}\,dx$. We observe that the formulation is well-posed only if $N \le M$. We further observe that for any $r_{\text{Gauss}} > 0$ and $x_m^{\text{obs}} \in \Omega$, $\ell_m^o \in \mathcal{Y}'$. Here, the observation centers $\{x_m^{\text{obs}}\}_{m=1}^M \subset \Omega$ are selected using the SGreedy-

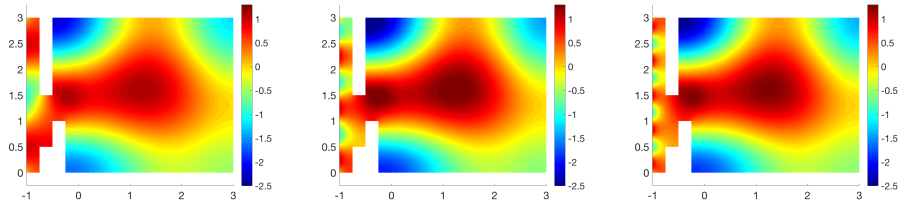

(a) $h^{\text{true}} = h_1$, $\mu = 2$ (b) $h^{\text{true}} = h_2$, $\mu = 2$ (c) $h^{\text{true}} = h_3$, $\mu = 2$

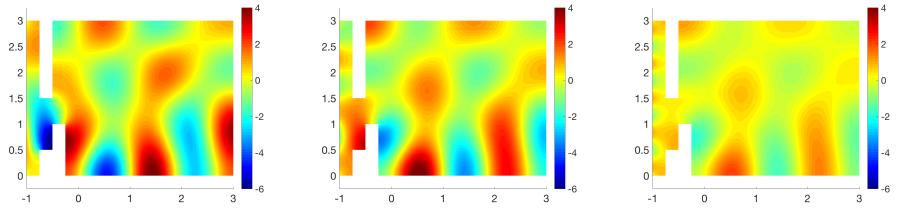

(d) $h^{\text{true}} = h_1$, $\mu = 4$ (e) $h^{\text{true}} = h_2$, $\mu = 4$ (f) $h^{\text{true}} = h_3$, $\mu = 4$

Fig. 4: Application to state estimation: visualization of the real part of the true field $\text{Re}\{u^{\text{true}}(\mu)\}$ for $\Omega^{\text{pb},2}$.

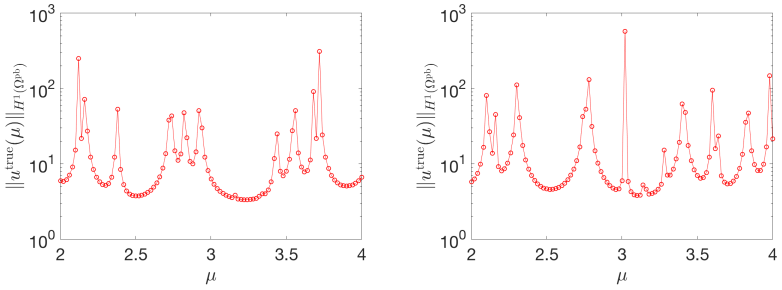

(a) $\Omega^{\text{pb},1}$ (b) $\Omega^{\text{pb},2}$

Fig. 5: Application to state estimation: behavior of $\|u^{\text{true}}(\mu)\|_{H^1(\Omega^{\text{pb}})}$ with μ, for $\Omega^{\text{pb},1}$ and $\Omega^{\text{pb},2}$, and for $h^{\text{true}} = h_1$.

plus algorithm with tolerance $tol = 0.2$ (see [36, Algorithm 3.2.1]).

It is possible to show that $\eta^\star = \sum_{m=1}^M \eta_m R_{\mathcal{Y}} \ell_m^o \in \mathcal{Y}_M := \text{span}\{R_{\mathcal{Y}} \ell_m^o\}_{m=1}^M$, $\boldsymbol{\eta} \in \mathbb{C}^M$, where $R_{\mathcal{Y}} \ell_m^o \in \mathcal{Y}$ is the Riesz element associated with the functional ℓ_m^o, $m = 1, \ldots, M$. Substituting this expression for η in (19), we can compute $u^\star$ by solving a linear system of size $N + M$. Furthermore, if we introduce the stability constant $\beta_{N,M} := \inf_{z \in \mathcal{Z}_N} \sup_{q \in \mathcal{Y}_M} \frac{(z,q)_{\mathcal{Y}}}{\|z\|_{\mathcal{Y}} \|q\|_{\mathcal{Y}}}$, we can state the following *a priori* error estimate (see [4, Remark 2.12] for the proof):

$$\|u^{\text{true}} - u^\star\|_{\mathcal{Y}} \leq \frac{1}{\beta_{N,M}} \inf_{\eta \in \mathcal{Y}_M \cap \mathcal{Z}_N^\perp} \inf_{z \in \mathcal{Z}_N} \|u^{\text{true}} - z - \eta\|_{\mathcal{Y}}. \tag{20}$$

We observe that $\beta_{N,M} \equiv 0$ for $N > M$ and $\frac{1}{\beta_{N,M}}$ increases as N increases (i.e., more measurements are required to stabilise the formulation), while $\inf_{\eta \in \mathcal{Y}_M \cap \mathcal{Z}_N^\perp} \inf_{z \in \mathcal{Z}_N} \|u^{\text{true}} - z - \eta\|_{\mathcal{Y}}$ decreases as N increases: this shows the importance of rapidly convergent spaces $\{\mathcal{Z}_N\}_N$.

By applying Algorithm 1, we can generate rapidly convergent spaces $\{\mathcal{Z}_N\}_N$ for the manifold $A(\mathcal{T})$. We here consider $\mathcal{Y} = H^1(\Omega)$, $\mathcal{V} = H^1(\Omega^{\text{bk}})$, and $\mathcal{T} = H^{1/2}(\Gamma^{\text{in}})$ endowed with the inner products:

$$(u, v)_{\mathcal{Y}} = \int_\Omega \nabla u \cdot \nabla \bar{v} + u\bar{v}\, dx, \quad \forall\, u, v \in \mathcal{Y}; \tag{21a}$$

$$(u, v)_{\mathcal{V}} = \int_{\Omega^{\text{bk}}} \nabla u \cdot \nabla \bar{v} + u\bar{v}\, dx, \quad \forall\, u, v \in \mathcal{V}; \tag{21b}$$

and

$$(u, v)_{\mathcal{T}} = (E^{\text{in}}(u), E^{\text{in}}(v))_{\mathcal{V}}, \quad \text{s.t.} \quad \begin{cases} -\Delta E^{\text{in}}(u) + E^{\text{in}}(u) = 0 & \text{in } \Omega^{\text{bk}} \\ \partial_n E^{\text{in}}(u) = 0 & \text{on } \partial\Omega^{\text{bk}} \setminus \Gamma^{\text{in}} \\ E^{\text{in}}(u) = u & \text{on } \Gamma^{\text{in}} \end{cases} \tag{21c}$$

4.3. Numerical results.

4.3.1. The case $\mathcal{P} = \{\bar{\mu}\}$. We first consider the case in which the value of μ in (16) is known *a priori*. We consider a $\mathcal{N}_{\text{in}} = 20$-dimensional discretization of the input space $\mathcal{T}$ based on Legendre polynomials, and we apply a standard dense eigensolver to compute the eigenvalues and eigenvectors of (4). We remark that, since the bk model is independent of the particular choice of Ω^{pb}, we generate a single hierarchy of approximation spaces for both $\Omega^{\text{pb},1}$ and $\Omega^{\text{pb},2}$. We further observe that the discretization of $\mathcal{T}$ implicitly filters out high-order modes on Γ^{in}.

Figure 6(a) shows the behavior of $\sqrt{\lambda_{N+1}^{\mathcal{N}_{\text{in}}}}$ with N for three different values of $\bar{\mu}$, while Figures 6(b) and 6(c) show the behavior of the relative H^1 best-fit error

$$E_N^{\text{rel}} = \max_{k=1,2,3} \frac{\|u_k^{\text{true}}(\bar{\mu}) - \Pi^{\mathcal{Y}}_{\mathcal{Z}_N^{\text{te},\mathcal{N}_{\text{in}}}} u_k^{\text{true}}(\bar{\mu})\|_{\mathcal{Y}}}{\|u_k^{\text{true}}(\bar{\mu})\|_{\mathcal{Y}}} \tag{22}$$

for $\Omega^{\text{pb}} = \Omega^{\text{pb},1}$ and $\Omega^{\text{pb}} = \Omega^{\text{pb},2}$, respectively, where $u_k^{\text{true}}(\bar{\mu})$ is the solution to (16) for $h^{\text{true}} = h_k$. We observe that $\sqrt{\lambda_{N+1}^{\mathcal{N}_{\text{in}}}} \gtrsim E_N^{\text{rel}}$: this is in good agreement with the result in Proposition 3.3. We also observe that the transfer eigenvalues increase as $\bar{\mu}$ increases: this is in good agreement with the discussion in [36, Chapter 5.1.2].

Figure 7 compares the behavior of the global POD eigenvalues associated with $\{\widehat{A}(g_n; \bar{\mu})\}_{n=1}^{\mathcal{N}_{\text{in}}}$ based on the $\mathcal{V}$ inner product with the transfer eigenvalues for $\bar{\mu} = 2$ and $\bar{\mu} = 4$. We observe that the decay of the global POD eigenvalues is significantly slower than the decay of the transfer eigenvalues. This confirms that while the global manifold $\widehat{A}(\mathcal{T})$ cannot in general be approximated through a low-dimensional reduced space, the local manifold is reducible.

In Figure 8, for $\bar{\mu} = 2$ we compare the approximation properties of the empirical basis generated using our method with the approximation properties of the polynomial space

$$\mathcal{Z}_N^{\text{leg}} := \text{span}\left\{ (L_{i-1}(x_1) + \alpha_i L_i(x_1))\,(L_{j-1}(x_2) + \alpha_j L_j(x_2)) :\ 1 \le i, j \le \sqrt{N} \right\}, \tag{23}$$

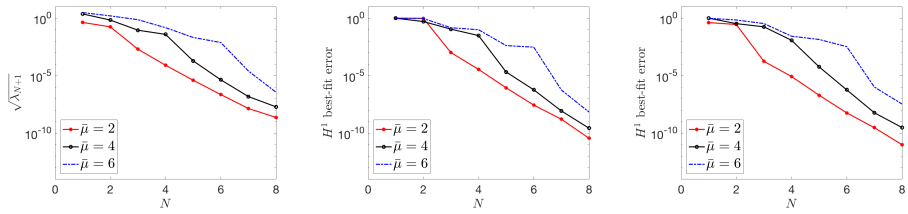

(a) (b) $\Omega^{\rm pb,1}$ (c) $\Omega^{\rm pb,2}$

Fig. 6: Application to state estimation: transfer eigenproblem. Behavior of $\sqrt{\lambda^{\mathcal{N}_{\rm in}}_{N+1}}$ (Figure (a)), and of the H^1 best-fit error (22) for three values of $\bar{\mu}$, and for $\Omega^{\rm pb,1}$ (Figure (b)) and $\Omega^{\rm pb,2}$ (Figure (c)) ($\mathcal{N}_{\rm in} = 20$).

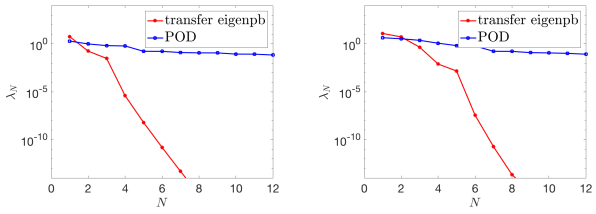

(a) $\bar{\mu} = 2$ (b) $\bar{\mu} = 4$

Fig. 7: Application to state estimation: transfer eigenproblem. Eigenvalues of the global POD, and eigenvalues of the transfer eigenproblem, for two values of $\bar{\mu}$.

where $\{L_i\}_{i=0}^{\sqrt{N}}$ are the one-dimensional Legendre polynomials, and $\{\alpha_i\}_{i=1}^{\sqrt{N}}$ are chosen such that $\partial_n \zeta_{i,j} = 0$ on $\partial\Omega \cap \partial\Omega^{\rm bk}$. As expected from the theory, our empirical basis outperforms the Legendre basis.

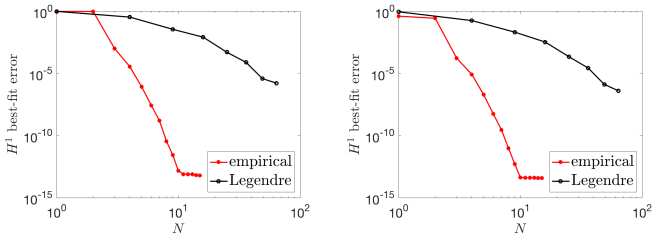

(a) $\Omega^{\rm pb,1}$ (b) $\Omega^{\rm pb,2}$

Fig. 8: Application to state estimation: behavior of the relative H^1 errors for the empirical space and for the Legendre space (23) ($\bar{\mu} = 2$).

In Figure 9(a), we compute the relative best-fit error associated with the field $u_{g_k^\star}(\bar{\mu})|_\Omega$ where $g_k^\star(x_2) = e^{k|x_2 - 1.5|}$ for $k = 1, 2, 3$. Unlike in the previous cases,

the Dirichlet datum is directly imposed on Γ^{in}. Since $g_k^\star$ is not a polynomial, the approximation properties of the transfer eigenspaces should be polluted by the error in the input (cf. (13)):

$$\frac{\|\Pi^{\mathcal{T}}_{\mathcal{T}^\perp_{\mathcal{N}_{\text{in}}}} g_k^\star\|_{\mathcal{T}}}{\|g_k^\star\|_{\mathcal{T}}} = \begin{cases} 0.0132 & k=1, \\ 0.0068 & k=2, \\ 0.0024 & k=3. \end{cases}$$

Results show that also in this case the relative H^1 error E_N converges extremely fast with N, and is well-below the relative discretization error $\|\Pi^{\mathcal{T}}_{\mathcal{T}^\perp_{\mathcal{N}_{\text{in}}}} g_k^\star\|_{\mathcal{T}}/\|g_k^\star\|_{\mathcal{T}}$. To explain the rapid convergence for rough boundary data, recalling (13), we compute the operator norm $\|A\|_{\mathcal{L}(\mathcal{T}^\perp_{\mathcal{N}_{\text{in}}},\mathcal{Y})}$ with $\mathcal{N}_{\text{in}}$ for the same three values of $\bar{\mu}$: we observe exponential convergence in $\mathcal{N}_{\text{in}}$. This shows that highly-oscillatory modes on Γ_{in} decay extremely fast in the interior of the domain, and ultimately motivates the use of Legendre polynomials to discretize the input space.

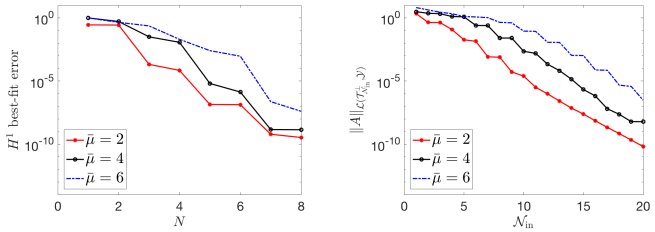

(a) (b)

Fig. 9: Application to state estimation. Figure (a): behavior of the relative H^1 errors for the empirical space for rough data ($g_k^\star(x_2) = e^{k|x_2-1.5|}$, $\mathcal{N}_{\text{in}} = 20$). Figure (b): behavior of the operator norm $\|A\|_{\mathcal{L}(\mathcal{T}_{\mathcal{N}_{\text{in}}},\mathcal{Y})}$ with $\mathcal{N}_{\text{in}}$ for three values of μ.

Figure 10 shows the performance of the data assimilation procedure. To assess performance, we consider both L^2 and H^1 maximum relative error over the three choices of the Dirichlet datum $h_k(x_2) = \sin(\pi k x_2)$, $k = 1, 2, 3$. By comparing Figures 10 with Figures 6(b) and 6(c), we observe that, for $M \simeq N$, the state estimation error is of the same order as $\|u^{\text{true}} - \Pi^{\mathcal{Y}}_{\mathcal{Z}_N} u^{\text{true}}\|_{\mathcal{Y}}$ and then slowly decreases as M increases: this is in agreement with the *a priori* result (20), and empirically demonstrates the importance of considering accurate background spaces $\{\mathcal{Z}_N\}_N$ in the PBDW formulation. For the problem at hand, the rate of convergence with M is approximately $\mathcal{O}(M^{-1})$ in L^2 norm, and $\mathcal{O}(M^{-1/2})$ in H^1 norm.

4.3.2. The case $\mathcal{P} \neq \{\bar{\mu}\}$. We first study the behavior of the eigenvalues associated with the application of Algorithm 1. We here consider $n_{\text{train}} = 11$ equispaced training parameters $\{\mu^i\}_{i=1}^{n_{\text{train}}}$ in $\mathcal{P} = [2, 4]$, we set $\mathcal{N}_{\text{in}} = 20$, and we consider several values of N. Figure 11(a) shows the behavior of the transfer eigenvalues $\lambda_n^{\mathcal{N}_{\text{in}}}$ for different values of $\mu \in \mathcal{P} = [2, 4]$, while Figure 11(b) shows the behavior of the POD eigenvalues λ_J^{POD} with J for different choices of N. We observe exponential convergence of the POD eigenvalues. We further observe that POD eigenvalues are only weakly affected by the value N: this means that only the first few transfer eigenmodes for each value of μ contribute to the final background $\mathcal{Z}_N$. As observed in section

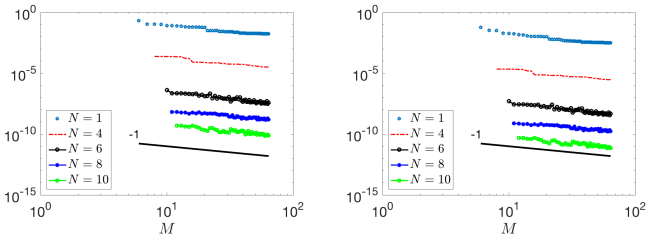

(a) L^2, $\Omega^{\text{pb},1}$ (b) L^2, $\Omega^{\text{pb},2}$

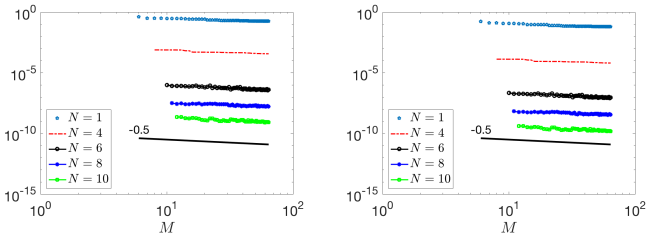

(c) H^1, $\Omega^{\text{pb},1}$ (d) H^1, $\Omega^{\text{pb},2}$

Fig. 10: Application to state estimation: behavior of the relative L^2 and H^1 errors ($\mu = 2$).

2.3, we could thus keep $\widetilde{N} > N$ POD modes in Algorithm 1. We also observe that $\lambda_n^{\text{POD}} \gg \max_i \lambda_n^{\mathcal{N}_{\text{in}},i}$ for sufficiently large n: this means that parameter variations dominate over variations in the boundary condition.

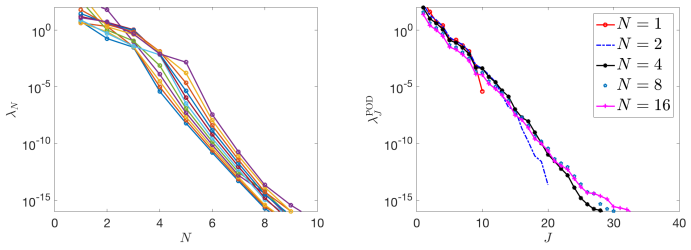

(a) (b)

Fig. 11: Application to state estimation: behavior of the eigenvalues computed in Algorithm 1. Figure (a): behavior of the transfer eigenvalues $\lambda_n^{\mathcal{N}_{\text{in}}}$ for different values of $\mu \in \mathcal{P}$. Figure (b): behavior of the POD eigenvalues λ_J^{POD} for different choices of N, $J = 1, \ldots, n_{\text{train}} \times N$ ($n_{\text{train}} = 11$, $\mathcal{N}_{\text{in}} = 20$).

Figure 12 shows the performance of the data assimilation procedure. To assess performance, we compute the H^1 maximum relative error (over Ω) for the two problem domains $\Omega^{\text{pb},1}$ and $\Omega^{\text{pb},2}$, for three choices of the Dirichlet datum $h_k(x_2) = \sin(\pi k x_2)$, $k = 1, 2, 3$, and $n_{\text{test}} = 5$ different values of μ in $\mathcal{P}$. To interpret the results, we also

report the behavior of the relative H^1 best-fit error. We observe that our procedure is able to generate an extremely accurate background space for the bk manifold $A(\mathcal{T})$, and thus for the true field.

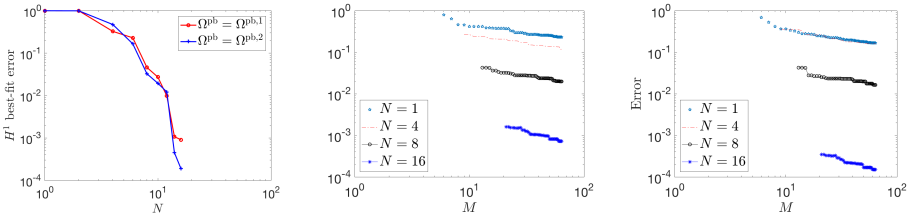

(a) (b) H^1 $\Omega^{\rm pb,1}$ (c) H^1 $\Omega^{\rm pb,2}$

Fig. 12: Application to state estimation: data assimilation results. Figure (a): behavior of the H^1 best-fit error with N. Figures (b) and (c): behavior of the PBDW relative H^1 error with M, for $\Omega^{\rm pb,1}$ and $\Omega^{\rm pb,2}$. ($n_{\rm train} = 11$, $\mathcal{N}_{\rm in} = 20$, $n_{\rm test} = 5$).

In Table 2, we report the overall computational cost associated with Algorithm 1 for $N = 15$, and $\mathcal{N}_{\rm in} = 20$. Simulations are performed on a Mac OS 2.8GHz Intel Core 7 with 16 GB memory. Reported times do not include the cost of generating the FE mesh and the FE matrices (roughly 0.7 seconds); the reported times for the transfer eigenproblem do include the cost of assembling the matrices $\mathbb{U}$ and $\mathbb{T}$ — the latter requires the computation of the extension $E^{\rm in}$, and is performed only once for all values of μ. We observe that the cost of the second POD is negligible.

	$\mathcal{N}_{\rm in} \times n_{\rm train}$ PDE solves	$n_{\rm train}$ TEs	1 POD	overall
$\Omega^{\rm pb,1}$	8.2	0.5	0.02	9.0 – 9.1
$\Omega^{\rm pb,2}$	8.2	0.5	0.02	9.0 – 9.1

Table 2: Application of Algorithm 1: computational times ($n_{\rm train} = 11$, $N = 15$, $\mathcal{N}_{\rm in} = 20$) in seconds.

5. Application to parameter estimation.

5.1. An acoustic waveguide. We apply our localization procedure in the context of parameter estimation. Figure 13(a) shows an acoustic waveguide with an expansion chamber. We assume that (i) the input is time-harmonic of known frequency, (ii) the material properties of the medium in $\Omega^{\rm bk} \setminus V^{\rm un}$ are known, and (iii) the material properties are unknown in $V^{\rm un}$. Our goal is to estimate the wavenumber κ in the region $V^{\rm un}$ inside the chamber based on local measurements of the acoustic pressure in the region V in Figure 13(b) — which is referred to as the *observable domain*. As in the previous example, we intend $\Omega^{\rm bk}$ to be part of a larger system to which is connected at the ports $\Gamma^{\rm in,1}$ and $\Gamma^{\rm in,2}$. We refer to Figure 13 for a quantitative description of the bk and observable domains.

In view of the mathematical definition of the inverse problem, we define the

mathematical model[3] (in non-dimensional form)

$$\text{(24a)} \qquad \begin{cases} -(1+\mathrm{i}\epsilon)\,\Delta u_g(\mu) - \kappa(\mu)^2 u_g(\mu) = 0 & \text{in } \Omega^{\rm bk}, \\ u_g(\mu) = g & \text{on } \Gamma^{\rm in} := \Gamma^{\rm in,1} \cup \Gamma^{\rm in,2}, \\ \partial_n u_g(\mu) = 0 & \text{on } \partial\Omega^{\rm bk} \setminus \Gamma^{\rm in}, \end{cases}$$

where $\epsilon = 10^{-4}$,

$$\text{(24b)} \qquad \kappa(x;\mu) := \begin{cases} 3 & \text{if } x \in \Omega^{\rm bk} \setminus V^{\rm un}, \\ 3\sqrt{\mu} & \text{if } x \in V^{\rm un}, \end{cases}$$

and $\mu \in \mathcal{P} = [0.5, 2]$. We further define the M observation functionals $\ell^o_m(v) = \ell(v, x^{\rm obs}_m, r_{\rm Gauss}) + \varepsilon_m$: here, $\varepsilon_1, \ldots, \varepsilon_M$ are M independent identically distributed (iid) Gaussian random variables with zero mean and variance $\sigma^2 = 0.1^2$; on the other hand, ℓ is given by

$$\text{(25)} \qquad \ell(v;\, x, r_{\rm Gauss}) := C(x) \int_V v(y) \exp\left(-\frac{|y-x|^2}{2r^2_{\rm Gauss}}\right) dy,$$

where $\{x^{\rm obs}_m\}_{m=1}^M \subset V$, $r_{\rm Gauss} = 0.05$, and C is a normalization constant. We summarize the parameter estimation problem in the box below.

Given the M measurements $\ell^{\rm obs}_m := \ell^o_m(u_g(\mu)) + \varepsilon_m$ where $\mu \in \mathcal{P}$, $g \in \mathcal{T} := H^{1/2}(\Gamma^{\rm in})$, and $\varepsilon_m \overset{iid}{\sim} \mathcal{N}(0, \sigma^2)$, for $m = 1, \ldots, M$, estimate the value of μ.

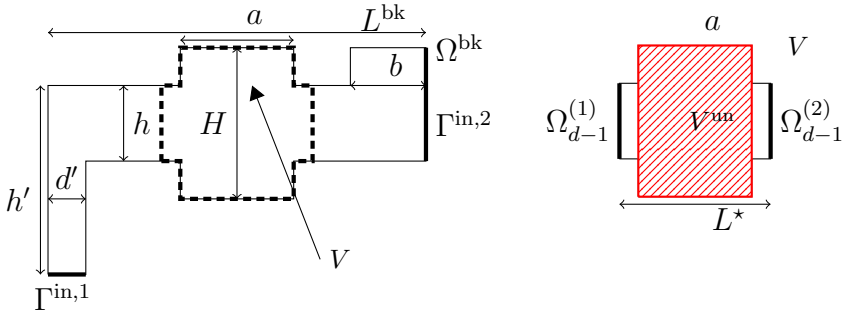

(a) bk domain (b) observable domain

Fig. 13: Application to parameter estimation: geometry ($h = 1$, $H = 2$, $L^{\rm bk} = 5$, $L^\star = 2$, $a = 1$, $h' = 2.5$, $d' = 0.5$, $b = 1$).

5.2. Formulation: a deterministic approach. In this work, we consider a deterministic approach to solve the inverse problem at hand. As we will discuss later, this requires the estimation of the pair (μ, g). Since the boundary condition g on $\Gamma^{\rm in}$ is unknown, the effective dimensionality of the inverse problem stated in the previous

[3] Unlike in the previous example, we here directly define the mathematical model in the bk domain. For this reason, we do not distinguish between true model and bk model.

section is extremely large. For this reason, we wish to reduce the dimensionality of the problem by resorting to the localization procedure proposed in this paper. With this in mind, we observe that for any $g \in \mathcal{T}$ and $\mu \in \mathcal{P}$, $u_g(\mu)|_V$ is the unique solution to the problem:

$$
\begin{cases}
-(1+\mathrm{i}\epsilon)\,\Delta u_{\bar{g}}(\mu) - \kappa(\mu)^2 u_{\bar{g}}(\mu) = 0 & \text{in } V \\
u_{\bar{g}}(\mu) = \bar{g} & \text{on } \Omega_{d-1} := \Omega_{d-1}^{(1)} \cup \Omega_{d-1}^{(2)} \\
\partial_n u_g(\mu) = 0 & \text{on } \partial V \setminus \Omega_{d-1},
\end{cases} \tag{26}
$$

where $\bar{g} = u_g(\mu)|_{\Omega_{d-1}}$, and $\Omega_{d-1} = \Omega_{d-1}^{(1)} \cup \Omega_{d-1}^{(2)} = \{|x_1| = L^\star/2\} \cap \partial V$ is defined in Figure 13.

By applying Algorithm 1, we can determine an effective parametrization for the Dirichlet datum $\bar{g}$ in (26): this leads to a dramatic reduction of the dimensionality of the inverse problem. We here choose $\mathcal{T} = H^{1/2}(\Gamma^{\text{in}})$, $\mathcal{V} = H^1(\Omega^{\text{bk}})$, $\mathcal{Y} = H^{1/2}(\Omega_{d-1})$ endowed with the inner products:

$$
(u,v)_{\mathcal{V}} = \int_{\Omega^{\text{bk}}} \nabla u \cdot \nabla \bar{v} + u\bar{v}\, dx, \quad \forall\, u, v \in \mathcal{V}, \tag{27a}
$$

(27b)

$$
(u,v)_{\mathcal{T}} = (E^{\text{in}}(u), E^{\text{in}}(v))_{\mathcal{V}}, \ \text{ s.t } \begin{cases}
-\Delta E^{\text{in}}(u) + E^{\text{in}}(u) = 0 & \text{in } \Omega^{\text{bk}} \\
\partial_n E^{\text{in}}(u) = 0 & \text{on } \partial\Omega^{\text{bk}} \setminus \Gamma^{\text{in}} \\
E^{\text{in}}(u) = u & \text{on } \Gamma^{\text{in}}
\end{cases},
$$

and

$$
(u,v)_{\mathcal{Y}} = (E^{\text{out}}(u), E^{\text{out}}(v))_{\mathcal{V}}, \ \text{ s.t } \begin{cases}
-\Delta E^{\text{out}}(u) + E^{\text{out}}(u) = 0 & \text{in } \Omega^{\text{bk}} \\
\partial_n E^{\text{out}}(u) = 0 & \text{on } \partial\Omega^{\text{bk}} \\
E^{\text{out}}(u) = u & \text{on } \Omega_{d-1}
\end{cases}. \tag{27c}
$$

If we denote by $\mathcal{Z}_N = \text{span}\{\zeta_n\}_{n=1}^N \subset \mathcal{Y}$ the reduced space obtained by applying Algorithm 1, we can state the optimization statement associated with our parameter estimation problem as follows: given the measurements $\{\ell_m^{\text{obs}}\}_{m=1}^M$, find $(\mu^\star, \mathbf{z}^\star) \in \mathcal{P} \times G \subset \mathbb{R} \times \mathbb{C}^N$ such that

$$
(\mu^\star, \mathbf{z}^\star) \in \arg \min_{(\mu,\mathbf{z}) \in \mathcal{P}\times G} \sum_{m=1}^M |\ell_m^{\text{obs}} - \ell_m^o(u_{\bar{g}_N}(\mu))|^2, \quad \text{subject to } \bar{g}_N = \sum_{n=1}^N z_n\, \zeta_n. \tag{28}
$$

Problem (28) is a nonlinear non-convex problem of real dimension $2N+1$. We resort to an off-the-shelf Matlab optimizer to solve (28). In more detail, we resort to `fmincon` ([23]), and we consider a sequential quadratic programming (SQP, see e.g. [6]) method for non-convex optimization. The gradient of the objective function is estimated through finite difference. Since the problem is non-convex, we consider ten initial conditions chosen randomly in $\mathcal{P} \times G$, and then we select $(\mu_j^\star, \mathbf{z}_j^\star)$, $j = 1, \ldots, 10$, that minimizes the objective. The numerical results are not particularly sensitive to the choice of G: in all our numerical simulations, we first solve a state estimation problem for $\bar{g}$ using only the observations on Ω_{d-1}, then we set $G = \{\mathbf{z} = \mathbf{x} + \mathrm{i}\mathbf{y} : x_n \in [\hat{x}_n \pm \frac{1}{2}\max(|\hat{x}_n|, \text{tol})], y_n \in [\hat{y}_n \pm \frac{1}{2}\max(|\hat{y}_n|, \text{tol})]\}$, where $\text{tol} = 1$, and $\hat{\mathbf{z}} = \hat{\mathbf{x}} + \mathrm{i}\hat{\mathbf{y}}$ is the vector of coefficients associated with the estimate of $\bar{g}$.

We appeal to a Finite Element solver[4] to generate the data $\{\ell_m^{\rm obs}\}_{m=1}^M$ and to compute the solution $u_{\bar{g}_N}(\mu)$ at each iteration of the optimization algorithm. Since the solution to (28) involves many evaluations of the objective, we envision that for more challenging problems model reduction techniques are necessary to reduce the computational burden. For the particular class of problems considered in this paper, the Reduced Basis method ([16, 29, 31]) can be employed to speed up computations.

5.3. Numerical results. Figure 14 shows the behavior of the eigenvalues computed in Algorithm 1. We set $n_{\rm train} = 15$, and we consider a $\mathcal{N}_{\rm in} = 40$-dimensional discretization of the input space $\mathcal{T}$ based on Legendre polynomials. Figure 14(a) shows the behavior of the transfer eigenvalues $\lambda_n^{\mathcal{N}_{\rm in}}$ for three different values of $\mu \in \mathcal{P}$, while Figure 14(b) shows the behavior of the POD eigenvalues $\lambda_J^{\rm POD}$ with J for different choices of N. As in section 4, we observe very rapid convergence of the eigenvalues. For $J \geq 5$, and for all values of N, $\lambda_J^{\rm POD} \leq 10^{-3}$: for this reason, in all our tests, we consider $N = 5$ in (28). Since our FE discretization has 98 degrees of freedom associated with Ω_{d-1}, our localization procedure reduces the real dimension of the inverse problem from 197 to 11.

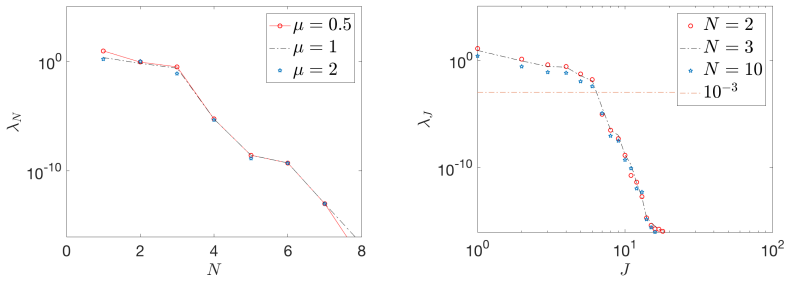

Fig. 14: Application to parameter estimation: behavior of the eigenvalues computed in Algorithm 1. Figure (a): behavior of the transfer eigenvalues $\lambda_n^{\mathcal{N}_{\rm in}}$ for three different values of $\mu \in \mathcal{P}$. Figure (b): behavior of the POD eigenvalues $\lambda_J^{\rm POD}$ for different choices of N, $J = 1, \ldots, n_{\rm train} \cdot N$ ($n_{\rm train} = 15$, $\mathcal{N}_{\rm in} = 30$).

Figure 15 shows the performance of the parameter estimation technique. In order to generate the data $\{\ell_m^{\rm obs} = \ell_m^o(u_g(\mu)) + \varepsilon_m\}_{m=1}^M \subset \mathbb{C}$, we here consider $\varepsilon \sim \mathcal{N}(0, \sigma^2)$ with $\sigma = 0.1$, eight different values of μ in $\mathcal{P}$, and two distinct Dirichlet boundary conditions on $\Gamma^{\rm in}$:

$$g_1(x) = \begin{cases} x_1 + \frac{1}{2}L_{\rm bk} & x \in \Gamma^{{\rm in},1}, \\ 1 + \sin(\pi x_2) & x \in \Gamma^{{\rm in},2}, \end{cases} \qquad g_2(x) = \begin{cases} 0 & x \in \Gamma^{{\rm in},1}, \\ \exp\left(-|x_2|\right) & x \in \Gamma^{{\rm in},2}. \end{cases}$$

Finally, we consider an uniform grid of $M = 36$ observations: Figure 15(a) shows the position of the observation sites $\{x_m^{\rm obs}\}_{m=1}^M$. Figures 15(b) and (c) show the results for $g = g_1$ and $g = g_2$, respectively. We observe that for all values of μ and for the two boundary conditions considered we are able to accurately estimate the value of μ: the relatively large number of measurements in V mitigates the effect of noise.

[4] We use a P8 FE discretization with $\mathcal{N}^{\rm bk} = 8417$ degrees of freedom in $\Omega^{\rm bk}$, $\mathcal{N} = 98$ degrees of freedom in Ω_{d-1}, and $\mathcal{N}^{\rm v} = 3713$ degrees of freedom in V.

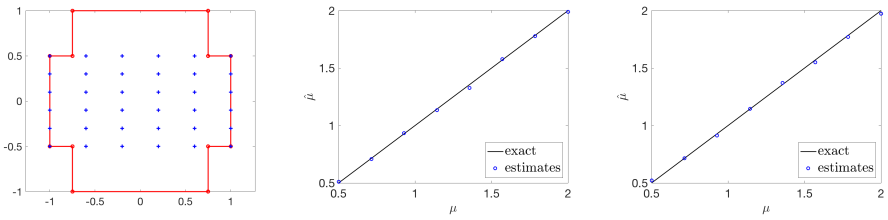

(a) (b) $g = g_1$ (c) $g = g_2$

Fig. 15: Application to parameter estimation: performance of the parameter estimation technique for two Dirichlet data g, and for several values of μ. Figure (a): observation centers $\{x_m^{\text{obs}}\}_m$ associated with the measurements. Figures (b) and (c): comparison between true and predicted value of the parameter μ.

6. Conclusions. We present a two-stage localization procedure for addressing data assimilation tasks in which the quantity of interest pertains to a subregion of the domain where the mathematical model is properly defined. The approach relies on a MOR procedure for the construction of local approximation spaces associated with parametric manifolds. In state estimation, given the domain of interest Ω, we employ the MOR technique to generate a background space $\mathcal{Z}_N$ associated with the domain of interest; the background is then employed to estimate the state based on local experimental measurements in the PBDW framework. In parameter estimation, we employ our MOR technique to determine a low-dimensional parametrization of the boundary conditions associated with the PDE in the observable domain V, and thus reduce the dimensionality of the inverse problem to be solved.

Theoretical and numerical results are presented to demonstrate the effectivity of our model reduction approach. If the uncertainty is confined to the boundary conditions of the PDE model, we proved that our approach is optimal in the sense of Kolmogorov for a wide class of linear inf-sup stable elliptic operators. In addition, numerical results for two acoustic problems demonstrate that, for moderate wave numbers, it is possible to generate accurate local approximation spaces even in the presence of high-dimensional uncertainty at the boundaries of the bk domain.

The localization strategy proposed in this paper can be applied to a wide class of data assimilation methods. In more detail, our localization procedure can be integrated with any state-estimation procedure that relies on projection-by-data (as opposed to projection-by-model). In parameter estimation, localization only aims at reducing the number of unknowns in the optimization statement; therefore, it can be incorporated in both deterministic and statistical approaches to inverse problems. As explained in the introduction, practical performance of the approach depends on the convergence of the Kolmogorov N-width, which should be assessed on a case-by-case basis.

We identify a number of open problems that are subject of ongoing research. From a theoretical perspective, we wish to study the optimality of our construction in the general case $\mathcal{P} \neq \{\bar{\mu}\}$. We wish also to extend our computational procedure and, more ambitiously, the analysis to nonlinear problems. Furthermore, we wish to develop a weak Greedy technique to adaptively select the parameters $\mu^1, \ldots, \mu^{n_{\text{train}}}$ for which solving the transfer eigenproblem: this will help us reduce the number of transfer

eigenproblems that should be solved during the offline stage. In this respect, we recall that efficient Greedy techniques rely on inexpensive *a posteriori* error estimators that are currently unavailable in this framework. From the engineering perspective, we wish to demonstrate the applicability of our technique to more realistic engineering applications.

Appendix A. Theoretical remarks. We present two theoretical results related to the discussion in section 3.

PROPOSITION A.1. *(**Relation between** (9b) **and** (10)) Let $\widetilde{\mathcal{T}}$ be the ball of radius C in $\mathcal{T}$, let $A : \mathcal{T} \to \mathcal{Y}$ be a linear continuous operator, and let us consider the bk manifold $\mathcal{M} = A(\widetilde{\mathcal{T}})$. Then,*

$$Z_N^{\rm kolm} \in \arg \inf_{Z_N \subset \mathcal{Y},\, \dim Z_N = N} \sup_{u \in \mathcal{M}} \|u - \Pi^{\mathcal{Y}}_{Z_N} u\|_{\mathcal{Y}}.$$

Furthermore, $\bar{d}_N(\mathcal{M}) = C\, d(A(\mathcal{T}))$.

Proof. Since $A - \Pi^{\mathcal{Y}}_{Z_N} A : \mathcal{T} \to \mathcal{Y}$ is a linear operator, we have

$$\begin{aligned} Z_N^{\rm kolm} \in &\arg \left(\inf_{Z_N \subset \mathcal{Y},\, \dim Z_N = N} \sup_{g \in \mathcal{T}} \frac{\|A(g) - \Pi^{\mathcal{Y}}_{Z_N} A(g)\|_{\mathcal{Y}}}{\|g\|_{\mathcal{T}}} \right) \\ = &\arg \left(\inf_{Z_N \subset \mathcal{Y},\, \dim Z_N = N} \sup_{g \in \mathcal{T}, \|g\|_{\mathcal{T}} = C} \frac{\|A(g) - \Pi^{\mathcal{Y}}_{Z_N} A(g)\|_{\mathcal{Y}}}{C} \right) \\ = &\arg \frac{1}{C} \left(\inf_{Z_N \subset \mathcal{Y},\, \dim Z_N = N} \sup_{g \in \mathcal{T}, \|g\|_{\mathcal{T}} \le C} \|A(g) - \Pi^{\mathcal{Y}}_{Z_N} A(g)\|_{\mathcal{Y}} \right) \end{aligned}$$

Since C is constant, recalling the definition of $\mathcal{M}$, this proves the first statement of the proof. The second statement can be shown using the same argument. ∎

PROPOSITION A.2. *(**Sufficient conditions for compactness**) Let $\Omega^{\rm bk} \subset \mathbb{R}^d$ be a d-dimensional Lipschitz domain, let $\Gamma^{\rm in} \subset \partial\Omega^{\rm bk}$ be an open set. Let $\Omega \subset \overline{\Omega}^{\rm bk}$ be either (i) a d-dimensional open set, or (ii) a $(d-1)$-dimensional open set such that there exists a d-dimensional Lipschitz domain $\Omega^\star \subset \Omega^{\rm bk}$ which satisfies $\Omega \subset \partial\Omega^\star$. Let us introduce the space $\mathcal{V} = H^s(\Omega^{\rm bk})$, the space $\mathcal{T} = H^{s-1/2}(\Gamma^{\rm in})$, and the space $\mathcal{Y}$ to be either $H^s(\Omega)$ if Ω is d-dimensional or $H^{s-1/2}(\Omega)$ if Ω is $(d-1)$-dimensional, where $s \ge 1$.*

Let the following hypotheses hold.

- *(*geometry*) The domains Ω and $\Gamma^{\rm in}$ satisfy the condition*

$$\operatorname{dist}(\overline{\Omega}, \overline{\Gamma}^{\rm in}) = \min_{x \in \overline{\Omega}} \min_{y \in \overline{\Gamma}^{\rm in}} \|x - y\|_2 > 0. \tag{29}$$

- *(*solution operators*) The operator $\widehat{A} : \mathcal{T} \to \mathcal{V}$ is linear and continuous, $\widehat{A} \in \mathcal{L}(\mathcal{T}, \mathcal{V})$; the bilinear form $\mathcal{G} : \mathcal{V} \times \mathcal{V}_0 \to \mathbb{R}$ is continuous; and for any d-dimensional domain $\Omega^\star \subset \Omega^{\rm bk}$, $\operatorname{dist}(\overline{\Omega}^\star, \overline{\Gamma}^{\rm in}) > 0$, there exists $C = C(\Omega, \Omega^\star) > 0$ such that for any $g \in \mathcal{T}$*

$$\|\widehat{A}(g)\|_{H^s(\Omega^\star)} \le C(\Omega^{\rm bk}, \Omega^\star) \|\widehat{A}(g)\|_{H^{s-1}(\Omega^{\rm bk})}. \tag{30}$$

Then, the operator A is compact from $\mathcal{T}$ to $\mathcal{Y}$.

Proof. We must show that given the sequence $\{g_n\}_n \subset \mathcal{T}$, $\|g_n\|_{\mathcal{T}} \leq C$, then the sequence $\{A(g_n)\}_n$ admits a strongly convergent subsequence in $\mathcal{Y}$. Recalling that $\widehat{A} \in \mathcal{L}(\mathcal{T}, \mathcal{V})$, the sequence $\{\widehat{A}(g_n)\}_n$ is bounded in $\mathcal{V}$. Then, due to the Banach Alaoglu theorem (see, e.g., [32, Theorem 6.12]), there exists a subsequence $\{\widehat{A}(g_{n_m})\}_m$ that converges weakly to $\bar{u} \in \mathcal{V}$. Recalling the definition of weak convergence, and recalling that for any $\phi \in \mathcal{V}_0$, $\mathcal{G}(\cdot, \phi) \in \mathcal{V}'$, we have that

$$0 = \mathcal{G}\left(\widehat{A}(g_{n_m}), \phi\right) \to \mathcal{G}\left(\bar{u}, \phi\right) = 0 \qquad \forall\, \phi \in \mathcal{V}_0.$$

This implies that $\bar{u} = \widehat{A}(\bar{u}|_{\Gamma^{\text{in}}})$. Then, exploiting (30), we find that for any $\Omega^\star \subset \Omega^{\text{bk}}$, dist $(\overline{\Omega}^\star, \overline{\Gamma}^{\text{in}}) > 0$,

$$\|\bar{u} - \widehat{A}(g_{n_m})\|_{H^s(\Omega^\star)} \leq C(\Omega^{\text{bk}}, \Omega^\star)\|\bar{u} - \widehat{A}(g_{n_m})\|_{H^{s-1}(\Omega^{\text{bk}})}.$$

Since $\mathcal{V} = H^s(\Omega^{\text{bk}})$ is compactly embedded in $H^{s-1}(\Omega^{\text{bk}})$ (see, e.g., [30, Theorem 1.3.5]), $\|\bar{u} - \widehat{A}(g_{n_m})\|_{H^{s-1}(\Omega^{\text{bk}})}$ converges to 0 as $m \to \infty$. As a result, $\widehat{A}(g_{n_m})|_{\Omega^\star} \to \bar{u}|_{\Omega^\star}$ in $H^s(\Omega^\star)$.

In order to complete the proof, we must distinguish two cases. If $\Omega \subset \mathbb{R}^d$, then thesis follows by substituting $\Omega^\star = \Omega$ and observing that $\|\bar{u} - \widehat{A}(g_{n_m})\|_{H^s(\Omega)} = \|\bar{u} - A(g_{n_m})\|_{\mathcal{Y}}$. On the other hand, if $\Omega \subset \mathbb{R}^{d-1}$, thesis follows by considering $\Omega^\star$ such that $\Omega \subset \partial\Omega^\star$ and then invoking the continuity of the trace operator from $H^s(\Omega^\star)$ to $H^{s-1/2}(\Omega)$. ∎

We remark that the proof of Proposition A.2 follows the same argument of [2, Lemma A.1] and [34, Proposition B.2], although the latter are specialized to a specific class of problems. Exploiting Proposition A.2, given a particular bk model, we can assess whether or not the reduced space based on the transfer eigenmodes is optimal by verifying conditions (29), and (30). We observe that the former depends only on the geometry and can be trivially checked. On the other hand, it is possible to show that (30), known as *Caccioppoli's inequality*, is satisfied by the solution to (i) linear damped elastodynamics, (ii) Stokes flow, (iii) advection-diffusion-reaction equation, and (iv) Helmholtz equation. We refer to [36, Appendix C], [2, Lemma A.1], and [34, Lemma 3.4] for the proofs.

Acknowledgments. The authors thank Prof. Kathrin Smetana (University of Twente) and Prof. Masayuki Yano (University of Toronto) for fruitful discussions.

REFERENCES

[1] I. Babuška, U. Banerjee, and J. E. Osborn, *Generalized finite element methods — main ideas, results and perspective*, International Journal of Computational Methods, 1 (2004), pp. 67–103.

[2] I. Babuška and R. Lipton, *Optimal local approximation spaces for generalized finite element methods with application to multiscale problems*, Multiscale Modeling & Simulation, 9 (2011), pp. 373–406.

[3] G. Berkooz, P. Holmes, and J. L. Lumley, *The proper orthogonal decomposition in the analysis of turbulent flows*, Annual review of fluid mechanics, 25 (1993), pp. 539–575.

[4] P. Binev, A. Cohen, W. Dahmen, R. DeVore, G. Petrova, and P. Wojtaszczyk, *Data assimilation in reduced modeling*, SIAM/ASA Journal on Uncertainty Quantification, 5 (2017), pp. 1–29.

[5] D. T. Blackstock, *Fundamentals of physical acoustics*, John Wiley & Sons, 2000.

[6] P. T. Boggs and J. W. Tolle, *Sequential quadratic programming*, Acta numerica, 4 (1995), pp. 1–51.

[7] A. Buhr and K. Smetana, *Randomized local model order reduction*, arXiv preprint arXiv:1706.09179v1, (2017).
[8] G. Chardon, A. Cohen, and L. Daudet, *Sampling and reconstruction of solutions to the helmholtz equation*, arXiv preprint arXiv:1301.0237, (2013).
[9] A. Cohen and R. DeVore, *Approximation of high-dimensional parametric pdes*, Acta Numerica, 24 (2015), pp. 1–159.
[10] A. Cohen and R. DeVore, *Kolmogorov widths under holomorphic mappings*, IMA Journal of Numerical Analysis, 36 (2015), pp. 1–12.
[11] Y. Efendiev and T. Y. Hou, *Multiscale finite element methods: theory and applications*, vol. 4, Springer Science & Business Media, 2009.
[12] J. L. Eftang and A. T. Patera, *Port reduction in parametrized component static condensation: approximation and a posteriori error estimation*, International Journal for Numerical Methods in Engineering, 96 (2013), pp. 269–302.
[13] C. I. Goldstein, *A finite element method for solving helmholtz type equations in waveguides and other unbounded domains*, Mathematics of Computation, 39 (1982), pp. 309–324.
[14] B. Haasdonk, *Convergence rates of the pod–greedy method*, ESAIM: Mathematical Modelling and Numerical Analysis, 47 (2013), pp. 859–873.
[15] P. Henning and D. Peterseim, *Oversampling for the multiscale finite element method*, Multiscale Modeling & Simulation, 11 (2013), pp. 1149–1175.
[16] J. S. Hesthaven, G. Rozza, and B. Stamm, *Certified reduced basis methods for parametrized partial differential equations*, SpringerBriefs in Mathematics, (2015).
[17] C. Himpe, T. Leibner, and S. Rave, *Hierarchical approximate proper orthogonal decomposition*, arXiv preprint arXiv:1607.05210v3, (2017).
[18] T. Y. Hou and X.-H. Wu, *A multiscale finite element method for elliptic problems in composite materials and porous media*, Journal of computational physics, 134 (1997), pp. 169–189.
[19] D. B. P. Huynh, D. J. Knezevic, and A. T. Patera, *A static condensation reduced basis element method: approximation and a posteriori error estimation*, ESAIM: Mathematical Modelling and Numerical Analysis, 47 (2013), pp. 213–251.
[20] K. Kunisch and S. Volkwein, *Galerkin proper orthogonal decomposition methods for a general equation in fluid dynamics*, SIAM Journal on Numerical analysis, 40 (2002), pp. 492–515.
[21] Y. Maday, A. T. Patera, J. D. Penn, and M. Yano, *A parameterized-background data-weak approach to variational data assimilation: formulation, analysis, and application to acoustics*, International Journal for Numerical Methods in Engineering, 102 (2015), pp. 933–965.
[22] Y. Maday, A. T. Patera, J. D. Penn, and M. Yano, *PBDW state estimation: Noisy observations; configuration-adaptive background spaces; physical interpretations*, ESAIM: Proceedings and Surveys, 50 (2015), pp. 144–168.
[23] MATLAB, *version 9.0 (R2016a)*, The MathWorks Inc., Natick, Massachusetts, 2016.
[24] J. M. Melenk and I. Babuška, *The partition of unity finite element method: basic theory and applications*, Computer methods in applied mechanics and engineering, 139 (1996), pp. 289–314.
[25] A. Moiola, R. Hiptmair, and I. Perugia, *Plane wave approximation of homogeneous helmholtz solutions*, Zeitschrift für angewandte Mathematik und Physik, 62 (2011), pp. 809–837.
[26] A. Paul-Dubois-Taine and D. Amsallem, *An adaptive and efficient greedy procedure for the optimal training of parametric reduced-order models*, International Journal for Numerical Methods in Engineering, 102 (2015), pp. 1262–1292.
[27] A. Pinkus, *N-widths in Approximation Theory*, Springer Science & Business Media, 1985.
[28] M. Pollow, K.-V. Nguyen, O. Warusfel, T. Carpentier, M. Müller-Trapet, M. Vorländer, and M. Noisternig, *Calculation of head-related transfer functions for arbitrary field points using spherical harmonics decomposition*, Acta acustica united with Acustica, 98 (2012), pp. 72–82.
[29] A. Quarteroni, A. Manzoni, and F. Negri, *Reduced Basis Methods for Partial Differential Equations: An Introduction*, vol. 92, Springer, 2015.
[30] A. Quarteroni and A. Valli, *Numerical approximation of partial differential equations*, vol. 23, Springer Science & Business Media, 2008.
[31] G. Rozza, D. P. Huynh, and A. T. Patera, *Reduced basis approximation and a posteriori error estimation for affinely parametrized elliptic coercive partial differential equations*, Archives of Computational Methods in Engineering, 15 (2008), pp. 229–275.
[32] S. Salsa, *Partial differential equations in action: from modelling to theory*, Springer Science & Business Media, 2008.
[33] L. Sirovich, *Turbulence and the dynamics of coherent structures. part i: Coherent structures*,

Quarterly of applied mathematics, 45 (1987), pp. 561–571.

[34] K. Smetana and A. T. Patera, *Optimal local approximation spaces for component-based static condensation procedures*, SIAM Journal on Scientific Computing, 38 (2016), pp. A3318–A3356.

[35] T. Taddei, *An adaptive parametrized-background data-weak approach to variational data assimilation*, ESAIM: Mathematical Modelling and Numerical Analysis, 51 (2017), pp. 1827–1858.

[36] T. Taddei, *Model order reduction methods for data assimilation; state estimation and structural health monitoring*, PhD thesis, MIT, 2017.

[37] T. Taddei, S. Perotto, and A. Quarteroni, *Reduced basis techniques for nonlinear conservation laws*, ESAIM: Mathematical Modelling and Numerical Analysis, 49 (2015), pp. 787–814.

[38] S. Volkwein, *Model reduction using proper orthogonal decomposition*, Lecture Notes, Institute of Mathematics and Scientific Computing, University of Graz. see http://www. uni-graz. at/imawww/volkwein/POD. pdf, (2011).

[39] E. G. Williams, *Fourier acoustics: sound radiation and nearfield acoustical holography*, Academic press, 1999.